

AD-A080 131

DAYTON UNIV OHIO SCHOOL OF ENGINEERING

F/0 10/3

ANALYSIS OF SOLIDIFICATION IN A CYLINDRICAL ANNULUS WITH INTERN--ETC(U)

JUL 79 H E BANDOW, J N CRISP

F33615-77-C-2004

UNCLASSIFIED

UDR-TR-78-69

AFAPL-TR-79-2088

NL

| OF |  
AD  
A080131



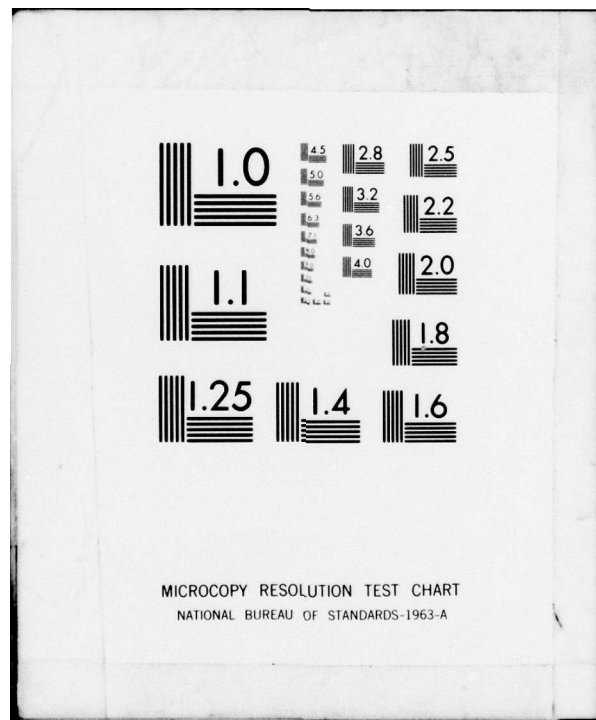
END

DATE

FILMED

3 - 80

DDC



ADA 080131

2 LEVEL II

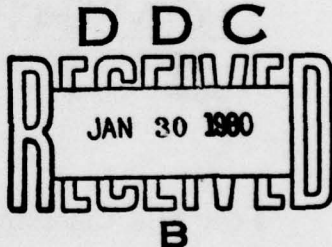
AFAPL-TR-79-2088

ANALYSIS OF SOLIDIFICATION IN A CYLINDRICAL ANNULUS WITH  
INTERNAL FINS

Howard E. Bandow  
John N. Crisp

School of Engineering  
University of Dayton  
Dayton, Ohio 45469

JULY 1979



TECHNICAL REPORT AFAPL-TR-79-2088  
Final Report for Period October 1977-October 1978

Approved for public release; distribution unlimited.

DDC FILE COPY

AIR FORCE AEROPROPULSION LABORATORY  
AIR FORCE WRIGHT AERONAUTICAL LABORATORIES  
AIR FORCE SYSTEMS COMMAND  
WRIGHT-PATTERSON AIR FORCE BASE, OHIO 45433

80 1 28 074

NOTICE

When Government drawings, specifications, or other data are used for any purpose other than in connection with a definitely related Government procurement operation, the United States Government thereby incurs no responsibility nor any obligation whatsoever; and the fact that the government may have formulated, furnished, or in any way supplied the said drawings, specifications, or other data, is not to be regarded by implication or otherwise as in any manner licensing the holder or any other person or corporation, or conveying any rights or permission to manufacture, use, or sell any patented invention that may in any way be related thereto.

This report has been reviewed by the Information Office (OI) and is releasable to the National Technical Information Service (NTIS). At NTIS, it will be available to the general public, including foreign nations.

This technical report has been reviewed and is approved for publication.

*Tom Mahefkey*

E. T. MAHEFKEY  
Project Engineer

*Robert R. Barthélémy*

ROBERT R. BARTHELEMY  
Chief, Energy Conversion Branch  
Aerospace Power Division

FOR THE COMMANDER

*Karl H. Muller*

KARL H. MULLER, Lt Colonel, USAF  
Deputy Director, Aerospace Power Division  
AF Aero Propulsion Laboratory

"If your address has changed, if you wish to be removed from our mailing list, or if the addressee is no longer employed by your organization please notify AFAPL/POE, W-PAFB, OH 45433 to help us maintain a current mailing list".

Copies of this report should not be returned unless return is required by security considerations, contractual obligations, or notice on a specific document.

Unclassified

SECURITY CLASSIFICATION OF THIS PAGE (When Data Entered)

| 19 REPORT DOCUMENTATION PAGE   |  |  | READ INSTRUCTIONS BEFORE COMPLETING FORM   |
|--|--|--|--|
| 1. REPORT NUMBER<br>18 AFAPL-TR-79-2088  | 2. GOVT ACCESSION NO.  | 3. RECIPIENT'S CATALOG NUMBER<br>9   | 4. TITLE (and Subtitle)<br>6 ANALYSIS OF SOLIDIFICATION IN A CYLINDRICAL ANNULUS WITH INTERNAL FINS. |
| 5. NAME OF REPORT & PERIOD COVERED<br>Final Report<br>October 1977-October 1978  |  | 6. SPONSORING ORGANIZATION NUMBER<br>UDR-TR-78-69 UDSE-TR-78-07  |  |
| 7. AUTHOR(s)<br>10 Howard E. Bandow, John N. Crisp   | 8. CONTRACT OR GRANT NUMBER(s)<br>15 F33615-77-C-2004, T25<br>3145-19-49   | 9. PERFORMING ORGANIZATION NAME AND ADDRESS<br>School of Engineering<br>University of Dayton<br>Dayton, Ohio 45469 | 10. PROGRAM ELEMENT, PROJECT, TASK AREA & WORK UNIT NUMBERS<br>16 3145 17 19                         |
| 11. CONTROLLING OFFICE NAME AND ADDRESS<br>Air Force Aero Propulsion Laboratory/POE<br>AFWAL (AFSC)<br>Wright-Patterson Air Force Base, Ohio 45433 | 12. REPORT DATE<br>11 July 1979  | 13. NUMBER OF PAGES<br>82 pages  | 14. MONITORING AGENCY NAME & ADDRESS (if different from Controlling Office)                          |
| 15. SECURITY CLASS. (of this report)<br>Unclassified   | 16a. DECLASSIFICATION/DOWNGRADING SCHEDULE<br>NA   | 17. DISTRIBUTION STATEMENT (of this Report)<br>Approved for public release; distribution unlimited.                | 18. DISTRIBUTION STATEMENT (if different from Report)  |
| 19. KEY WORDS (Continue on reverse side if necessary and identify by block number)<br>Heat transfer, heat pipes, thermal storage                   | 20. ABSTRACT (Continue on reverse side if necessary and identify by block number)<br>Solutions are presented for the one-dimensional and two-dimensional inward solidification of a material contained in a cylindrical annulus. The outer boundary is insulated and the inner boundary is subject to a constant efflux via a heat pipe. Results are presented for the axisymmetric case and for the cases of three and six longitudinal fins of rectangular cross section. The fins extend radially from inner to outer radius and were symmetrically | over   |  |

DD FORM 1 JAN 73 1473

Unclassified

SECURITY CLASSIFICATION OF THIS PAGE (When Data Entered)

409 377

50B

Unclassified

SECURITY CLASSIFICATION OF THIS PAGE(When Data Entered)

20. Abstract

spaced in the circumferential direction. The phase change material was LiF-MgF<sub>2</sub>-KF and was assumed to be initially at the fusion temperature.

Unclassified

SECURITY CLASSIFICATION OF THIS PAGE(When Data Entered)

## ABSTRACT

Solutions are presented for the one-dimensional and two-dimensional inward solidification of a material contained in a cylindrical annulus. The outer boundary is insulated and the inner boundary is subject to a constant efflux via a heat pipe. Results are presented for the axisymmetric case and for the cases of three and six longitudinal fins of rectangular cross section. The fins extend radially from inner to outer radius and were symmetrically spaced in the circumferential direction. The phase change material was LiF - MgF<sub>2</sub> - KF and was assumed to be initially at the fusion temperature.

|                                      |   |
|--------------------------------------|---|
| ACCESSION for                        |   |
| NTIS                                 | White Section <input checked="" type="checkbox"/> |
| DDC                                  | Buff Section <input type="checkbox"/>             |
| UNANNOUNCED <input type="checkbox"/> |   |
| JUSTIFICATION _____                  |   |
| BY _____                             |   |
| DISTRIBUTION/AVAILABILITY CODES      |   |
| Dist.                                | AVAIL. and/or SPECIAL                             |
| A                                    |   |

## TABLE OF CONTENTS

| <u>SECTION</u>       |  | <u>PAGE</u> |
|----------------------|--|-------------|
| I.                   | INTRODUCTION . . . . .                           | 1           |
| II.                  | OBJECTIVE AND SCOPE . . . . .                    | 3           |
| III.                 | SYSTEM DESCRIPTION. . . . .                      | 4           |
| VI.                  | ANALYTICAL APPROACH . . . . .                    | 8           |
| V.                   | ANALYSIS OF AXISYMMETRIC SYSTEM . . . . .        | 9           |
|                      | Formulation of Equations . . . . .               | 9           |
|                      | Solution . . . . .                               | 13          |
|                      | Approximate Analytical Solution . . . . .        | 13          |
|                      | Numerical Solution . . . . .                     | 14          |
| VI.                  | ANALYSIS OF FINNED SYSTEM. . . . .               | 18          |
|                      | Formulation of Equations . . . . .               | 18          |
|                      | Axisymmetric Formulation and Solution . . . . .  | 19          |
|                      | Finned System Formulation and Solution . . . . . | 22          |
| VII.                 | RESULTS AND DISCUSSION . . . . .                 | 25          |
|                      | Results with Axisymmetric Case. . . . .          | 25          |
|                      | Results with Fins . . . . .                      | 28          |
| VIII.                | SUMMARY AND CONCLUSIONS . . . . .                | 44          |
| IX.                  | RECOMMENDATIONS . . . . .                        | 45          |
| APPENDIX             |  |             |
| A                    | AXISYMMETRIC HEAT CONDUCTION EQUATION . . . . .  | 47          |
| B                    | PROGRAM ICE2 . . . . .                           | 51          |
| C                    | PROGRAM ENTH . . . . .                           | 57          |
| D                    | PROGRAM FIN . . . . .                            | 63          |
| REFERENCES . . . . . |  | 72          |

## LIST OF ILLUSTRATIONS

| <u>FIGURE</u>   | <u>PAGE</u> |
|---|-------------|
| 1      Axisymmetric HP/TES System Geometry . . . . .  | 5           |
| 2      Finned HP/TES System Geometry . . . . .  | 7           |
| 3      Flow Chart of Temperature Model of<br>Asixymmetric HP/TES System . . . . .   | 16          |
| 4      Flow Chart for Enthalpy Model of Finned HP/TES<br>System . . . . .   | 24          |
| 5      Temperature Distribution as a Function of Radial<br>Position in HP/TES System (Axisymmetrical Case) . . .                      | 27          |
| 6      Wall Temperature and Interface Location in<br>HP/TES System . . . . .  | 29          |
| 7      Temperature Distribution in Axisymmetric HP/TES<br>System Determined Analytically and by Two<br>Numerical Techniques . . . . . | 30          |
| 8      Interface Radius vs. Angle for 0, 3 & 6 Fin<br>HP/TES Systems, Heat Extraction Rate = 0.25 kw . . .                            | 32          |
| 9      Wall Temperature vs. Angle for 0, 3 & 6 Fin<br>HP/TES Systems, Heat Extraction Rate = 0.25 kw . . .                            | 33          |
| 10     Interface Radius vs. Angle for 0, 3 & 6 Fin<br>HP/TES Systems, Heat Extraction Rate = 0.50 kw . . .                            | 34          |
| 11     Wall Temperature vs. Angle for 0, 3 & 6 Fin<br>HP/TES Systems, Heat Extraction Rate = 0.50 kw . . .                            | 35          |
| 12     Interface Radius vs. Angle for 0 and 6 Fin HP/TES<br>Units, Heat Extraction Rate = 0.75 kw . . . . .                           | 36          |
| 13     Wall Temperature vs. Angle for 0 and 6 Fin HP/TES<br>Units, Heat Extraction Rate = 0.75 kw . . . . .                           | 37          |
| 14     Interface Radius vs. Angle for 0, 3 & 6 Fin HP/TES<br>Units, Heat Extraction Rate = 1.00 kw . . . . .                          | 38          |

LIST OF ILLUSTRATIONS (continued)

| <u>FIGURE</u> |   | <u>PAGE</u> |
|---------------|---|-------------|
| 15            | Wall Temperature vs. Angle for 0, 3 & 6 Fin<br>HP/TES Units, Heat Extraction Rate = 1.00 kw . . . . . | 39          |
| 16            | Interface Radius vs. Angle for 0, 3 & 6 Fin HP/TES<br>Units, Heat Extraction Rate = 1.50 kw . . . . . | 40          |
| 17            | Wall Temperature vs. Angle for 0, 3 & 6 Fin<br>HP/TES Units, Heat Extraction Rate = 1.50 kw . . . . . | 41          |
| 18            | Heat Extracted vs. Wall Temperature for<br>0, 3 & 6 Fin HP/TES Units . . . . .                        | 42          |
| B-1           | Program ICE2 . . . . .  | 53          |
| B-2           | Control Cards . . . . .   | 56          |
| C-1           | Program ENTH . . . . .  | 59          |
| C-2           | Control Cards . . . . .   | 62          |
| D-1           | Program FIN . . . . .   | 65          |
| D-2           | Control Cards . . . . .   | 71          |

## NOMENCLATURE

|                          |  |
|--------------------------|--|
| B                        | Fin thickness, ft  |
| c                        | Specific heat of the salt, BTU/lbm $^{\circ}$ F  |
| f                        | Volume ratio of solid salt to cannister  |
| G                        | Fin length, ft   |
| $h_{s\ell}$              | Latent heat of fusion of salt, BTU/lbm   |
| h                        | Specific enthalpy, BTU/lbm   |
| k                        | Thermal conductivity of salt, BTU/ft-hr- $^{\circ}$ F  |
| $k_1, k_2$<br>$k_3, k_4$ | Thermal conductivities on the element surfaces; $r=r_i+\Delta r/2$ ,<br>$\psi=\psi_i+\Delta\psi/2$ , $r=r_i-\Delta r/2$ , $\psi=\psi_i-\Delta\psi/2$ |
| $k_f$                    | Thermal conductivity of heat pipe wall, BTU/ft-hr- $^{\circ}$ F  |
| L                        | Radius of liquid solid interface, ft   |
| $L_f$                    | Radius of liquid solid interface when solidification is complete, ft   |
| $\ell$                   | Dimensionless frontal radius   |
| $\ell_f$                 | Dimensionless radius when solidification is complete   |
| h                        | Unit vector normal to the surface and directed outward from the control volume   |
| P                        | Thickness of heat pipe wall, ft  |
| q''                      | Heat flux rate, BTU/ft <sup>2</sup> -hr  |
| R                        | Radial distance, ft  |
| $R_I$                    | Radius of outer surface of heat pipe, ft   |
| $R_O$                    | Inner radius of outer cannister wall, ft   |
| r                        | Dimensionless radius   |
| $ST_e$                   | Stefan Number  |
| T                        | Temperature, $^{\circ}$ F  |
| $T_F$                    | Fusion temperature of salt, $^{\circ}$ F   |
| $\Delta T$               | Temperature drop across heat pipe wall, $^{\circ}$ F   |
| t                        | Time, hr   |
| v                        | Dimensionless volume = volume/ $\pi R_I^2$   |

|          |  |
|----------|--|
| $\alpha$ | Thermal diffusivity of salt, $\text{ft}^2/\text{hr}$ |
| $\theta$ | Dimensionless temperature                            |
| $\delta$ | Density of salt, $\text{lbm}/\text{ft}^3$            |
| $\tau$   | Dimensionless time                                   |
| $\tau_f$ | Dimensionless time when solidification is complete   |
| $\psi$   | Angle from Fin centerline                            |

LIST OF TABLES

| <u>TABLE</u> |                                      | <u>PAGE</u> |
|--------------|--------------------------------------|-------------|
| 1            | HP/TES Material Properties . . . . . | 6           |
| 2            | Fin Effectiveness . . . . .          | 43          |

## SECTION I INTRODUCTION

In many applications, thermal energy is available in an intermittent form, and demand for this energy does not necessarily coincide with availability. Solar energy, for example, is not available at night, and similarly wind powered electrical systems function only when the wind velocity is adequate. Also, the greater cost of commercial electrical power during periods of peak demand is another application in which energy storage could be used to good advantage. For these reasons, systems which can economically store large quantities of thermal energy with suitable recovery on demand are of increasing interest.

There are numerous energy storage systems available, at present, such as batteries, hydrogen storage/heat engine, flywheels, etc. Systems utilizing the phase change of materials having a high latent heat of fusion are also being evaluated at present and are of particular interest because:

- 1) heat transfer occurs at nearly constant temperatures and
- 2) large quantities of thermal energy may be stored in a relatively small volume.

The basic problem with systems utilizing the phase change of materials is analytically determining the melting and solidifying characteristics of a given system. The problem is inherently nonlinear and other than a few exact solutions the problem must be solved using numerical or analogue techniques. Carslaw and Jaeger<sup>(1)</sup> discuss the few exact solutions available as well as some approximate solutions. Kreith and Romie<sup>(2)</sup> present solutions for the cases of uni-dimensional cylinders, spheres and semi-infinite solids for the condition that the temperature gradient in the solid on solidification is constant or that the velocity of the solid/liquid interface remains constant. Kreith and

Romie<sup>(2)</sup> also discuss analogue computer solutions for semi-infinite solids. The bulk of the problems involving phase change have been solved by numerical techniques and include a variety of applications and problems such as continuous casting of cylindrical ingots<sup>(3)</sup>, two-dimensional freezing including convection effects in the liquid region<sup>(4)</sup>, and axisymmetric semi-infinite hollow-cylinder with convective heat transfer at the inner radius<sup>(5)</sup>.

## SECTION II

### OBJECTIVE AND SCOPE

The purpose of this investigation is to determine the thermal characteristics of energy-storage systems utilizing a cylindrical annulus to contain a phase change material. The outer surface is insulated and the inner surface (a heat pipe) is subjected to a constant heat flux. Additionally the influence of longitudinal fins within the annulus, with regard to heat transfer characteristics, is to be assessed. The fins will be symmetrically positioned in the circumferential direction.

Since a solution to a problem in solidification is also a solution to the corresponding problem in melting only solidification will be considered. The system is of sufficient length, in conjunction with heat pipe characteristics, that axial gradients will be neglected. The phase change material will be assumed to have a distinct fusion temperature and initially the liquid is uniformly at the fusion temperature. Additionally the thermal properties will be assumed to be uniform within each phase and mean values will be used for each phase. Convection within the fluid as well as radiation within both phases will be neglected.

### SECTION III SYSTEM DESCRIPTION

The thermal storage system consists of a cannister surrounding a heat pipe. The annulus formed by the cannister and the heat pipe contains 4.1705 lb. of the thermal storage material which is LiF - MgF<sub>2</sub> - KF. The cannister and heat pipe walls are made of .065" thick 304 Stainless Steel. The outside diameters are 1.5" for the heat pipe and 3.0" for the cannister. The geometry of this configuration is illustrated in Figure 1. Thermal properties assumed for the materials are presented in Table I. In addition there are two finned configurations containing three and six fins of 1/16" thick 304 Stainless Steel. The fins are parallel to, and project radially outward from, the longitudinal axis of the heat pipe. The configurations with three and six fins contain 3.9985 lb. and 3.8742 lb. of the thermal storage material, respectively. The finned configurations are illustrated in Figure 2.

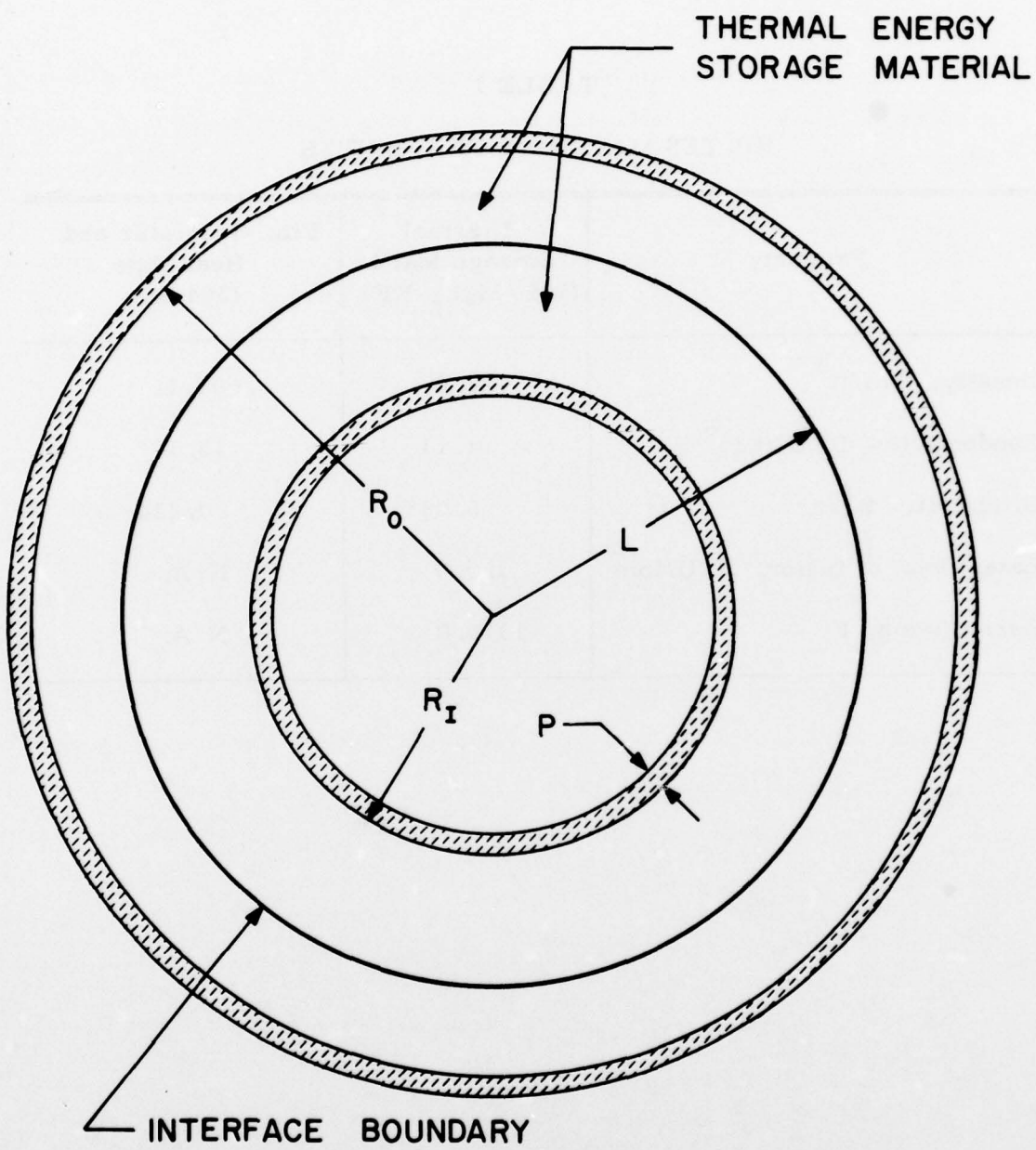


Figure 1. Axisymmetric HP/TES System Geometry

TABLE 1  
HP/TES MATERIAL PROPERTIES

| Property                               | Thermal Storage Mat'l<br>(LiF-MgF <sub>2</sub> -KF) | Fin, Cannister and Heat Pipe<br>(304 SS) |
|--|---|--|
| Density, lbm/ft <sup>3</sup>           | 181.0   | 501.12                                   |
| Conductivity, BTU/ft lb <sup>0</sup> F | 4.11  | 13.5                                     |
| Diffusivity, ft <sup>2</sup> /hr       | 0.035   | 0.224                                    |
| Latent heat of fusion, BTU/lbm         | 350.0   | N. A.                                    |
| Fusion temp, F                         | 1310.0  | N. A.                                    |

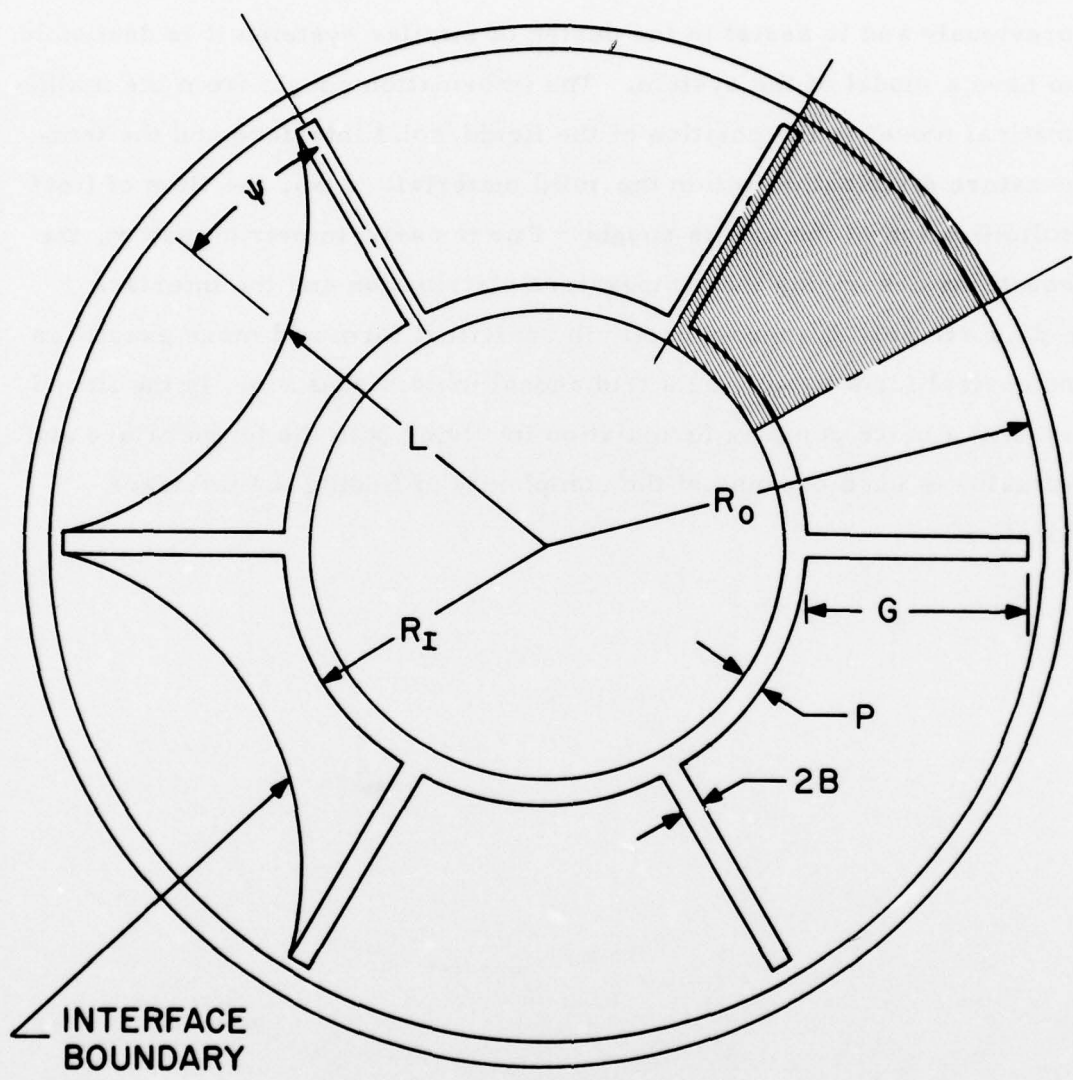


Figure 2. Finned HP/IES System Geometry

## SECTION IV

### ANALYTICAL APPROACH

In order to evaluate experimental data for the system described previously and to assist in the design of similar systems it is desirable to have a model of the system. The information sought from the mathematical model is the position of the liquid/solid interface and the temperature distribution within the solid material. Also, the time of final solidification of the salt is sought. For the axisymmetric system, the equations describing the temperature distribution and the interface radius are solved approximately in analytical form and more exactly in numerical form by solving a tridiagonal matrix equation. In the finned system a more complex formulation involving both the temperature and enthalpy is used because of the complexity of finding the interface location.

## SECTION V

### ANALYSIS OF AXISYMMETRIC SYSTEM

#### Formulation of Equations

In the axisymmetric model it is assumed that variations along the longitudinal axis of the system are negligible. Heat losses from the outer shell of the cannister are assumed negligible as is heat transfer by radiation between the hot outer portion of the system and the cold solidified salt. The entire system is assumed to be initially at the fusion temperature of the salt. The heat flux rate at the inner surface is assumed to be constant with respect to time and over the surface of the heat pipe. The change in internal energy of the heat pipe wall as heat is extracted from the system is ignored.

Under these assumptions the temperature distribution within the salt is governed by the unidimensional transient heat conduction equation:

$$\frac{\partial T}{\partial t} = \alpha \frac{\partial^2 T}{\partial R^2} + \frac{1}{R} \frac{\partial T}{\partial R} \quad (1)$$

where  $T$  = temperature, F

$t$  = time, hr

$R$  = radial distance, ft

$\alpha$  = thermal diffusivity of salt,  $\text{ft}^2/\text{hr}$

Equating the heat flux rate at the inner surface with the rate at which heat is conducted into a unit area of the surface yields:

$$k \frac{\partial T}{\partial R} = q'' \quad \text{for } R = R_I, t > 0 \quad (2)$$

where  $k$  = thermal conductivity of the salt, BTU/ft - hr - F

$q''$  = heat flux rate,  $\text{BTU}/\text{ft}^2 \cdot \text{hr}$

$R_I$  = radius of outer surface of heat pipe, ft

By assumption the initial temperature distribution is described by

$$T(R, t) = T_F \quad \text{for } R > R_I, t = 0 \quad (3)$$

where  $T_F$  = fusion temperature of salt, F.

Also, at the interface, the temperature is always at the fusion temperature:

$$T(R, t) = T_F \quad \text{for } R = L, t > 0 \quad (4)$$

where  $L$  = radius of liquid solid interface, ft.

Equations (1) through (4) constitute a partial differential equation of second order in space and first order in time along with the necessary initial condition and boundary conditions. However, since  $L$  is an unknown function of time, the problem is incomplete.

To determine  $L$ , two approaches are considered. In the first, the heat created by fusion at the interface is equated with the heat conducted from the interface to yield:

$$2\pi L \rho h_{s\ell} \frac{\partial L}{\partial t} = 2\pi L k \frac{\partial T}{\partial R} \quad \text{for } R = L, t > 0 \quad (5)$$

where  $\rho$  = density of salt,  $\text{lbm/ft}^3$

$h_{s\ell}$  = latent heat of fusion of salt,  $\text{BTU/lbm}$

Equation (5) along with the initial condition:

$$L(t) = R_I \text{ for } t = 0 \quad (6)$$

is sufficient to complete the formulation of the problem partially posed by Equations (1) through (4).

A second approach to determine  $L$  may be taken by equating the change in internal energy of the salt to the heat conducted out of the salt at the inner surface. This may be expressed as

$$\rho\pi(L^2 - R_I^2)h_{s\ell} - \int_{R_I}^{R=L} \rho c(T - T_F) 2\pi R dR = \dot{q}''t(2\pi R_I) \quad (7)$$

where  $c$  is the specific heat of the salt, BTU/lbm<sup>o</sup>F.

In Equation (7) the first term is the internal energy from fusion of the salt, the second term is the change in internal energy from the solid salt at the fusion temperature and the term on the right hand side is the heat extracted from the inner surface.

There will be a temperature drop across the heat pipe wall since heat is conducted across it. Since the change in internal energy of the wall is neglected this may be found from the steady state heat conduction equation to be:

$$\Delta T = \frac{\dot{q}'' R_I}{k_f} \ln \left\{ \frac{R_I}{R_I - p} \right\} \quad (8)$$

where  $\Delta T$  = temperature drop across heat pipe wall, F

$k_f$  = thermal conductivity of heat pipe wall, BTU/ft - hr - F

$p$  = thickness of heat pipe wall, ft.

Systems such as that described are seldom completely filled with solid salt in order to avoid excessive hydrostatic pressure since the salts are more dense in solid form than liquid. The ratio of the volume of solidified salt to the cannister volume may be written:

$$f = \frac{L_f^2 - R_I^2}{R_o^2 - R_I^2} \quad (9)$$

where  $f$  = volume ratio of solid salt to cannister

$R_o$  = inner radius of outer cannister wall, ft

$L_f$  = radius of liquid-solid interface when solidification is complete.

To generalize the solutions, it is desirable to express the preceding equations in terms of dimensionless variables. Substituting the variables

$$\theta = k(T - T_F)/\dot{q}''R_I; r = R/R_I; \ell = L/R_I; \tau = \alpha t/R_I^2 \quad (10)$$

into Equations (1) thru (7) yields, respectively

$$\frac{\partial^2 \theta}{\partial r^2} + \frac{1}{r} \frac{\partial \theta}{\partial r} = \frac{\partial \theta}{\partial \tau} \quad (11)$$

$$\frac{\partial \theta}{\partial r} = 1. \quad \text{for } r = 1, \tau > 0 \quad (12)$$

$$\theta(r, \tau) = 0. \quad \text{for } r > 1, \tau = 0 \quad (13)$$

$$\theta(r, \tau) = 0. \quad \text{for } r = \ell, \tau > 0 \quad (14)$$

$$\frac{\partial \ell}{\partial \tau} = S_{T_e} \frac{\partial \theta}{\partial r} \quad \text{for } r = \ell, \tau > 0 \quad (15)$$

$$\ell(\tau) = 1. \quad \tau = 0 \quad (16)$$

$$\frac{\ell^2 - 1}{2 S_{T_e}} - \int_1^\ell \theta r dr = \tau \quad (17)$$

Equation (16) may be solved for  $\ell$  to yield

$$\ell = \sqrt{1 + 2 S_{T_e} (\tau + \int_1^\ell \theta r dr)} \quad (18)$$

In Equations (15), (17), and (18):

$$S_{T_e} = \dot{q}''R_I/\alpha \rho h_s \ell \quad (19)$$

where  $S_{T_e}$  = Stefan Number

$\tau$  = dimensionless time

$\ell$  = dimensionless frontal radius

$r$  = dimensionless radius

$\theta$  = dimensionless temperature

It may be seen from Equations (11) through (16) that the solution for  $\theta$  and  $\ell$  in terms of  $r$  and  $\tau$  is characterized by the single dimensionless parameter  $ST_e$ . This is also true if Equation (18) is used rather than Equations (15) and (16) in conjunction with (11) through (14) to formulate the problem.

To find the time when solidification is complete, from Equation (9)

$$\ell_f = \sqrt{f \frac{(R_o^2 - R_I^2)}{R_I^2} + \frac{R_I^2}{R_I^2}} = \sqrt{1 + f(R_o^2 - R_I^2)} \quad (20)$$

and from Equation (17)

$$\tau_f = \frac{\ell_f^2 - 1}{2 ST_e} - \int_1^{\ell_f} \theta r dr \quad (21)$$

where  $\ell_f$  = dimensionless radius when solidification is complete

$\tau_f$  = dimensionless time when solidification is complete.

### Solution

Two different approaches to solving the system of equations representing the axisymmetric system will be considered. In the first, the change in internal energy of the solidified salt is neglected and an approximate analytical solution is found by solving Equations (11) through (15) subject to this assumption. To obtain the second solution, Equations (11) through (14) are expressed in finite difference form. The resulting tridiagonal matrix system is solved in conjunction with Equation (18) to find the temperature distribution and interface motion.

#### Approximate Analytical Solution

If the change in internal energy of the solid salt is neglected in comparison with the heat of fusion Equation (11) may be expressed:

$$\frac{\partial^2 \theta}{\partial r^2} + \frac{1}{r} \frac{\partial \theta}{\partial r} = 0 \quad (22)$$

Then the expression  $\theta = C_1 \ln r + C_2$  is seen to satisfy Equation (22). Applying the boundary conditions (12) and (14) gives the solution:

$$\theta = \ln \left( \frac{r}{\lambda} \right) \quad (23)$$

Substituting (23) into (15) yields

$$\frac{\partial \lambda}{\partial \tau} = \frac{S_{T_e}}{\lambda} \quad (24)$$

In Equation (24) we may separate variables and integrate to find an expression for  $\lambda$ :

$$\lambda = \sqrt{1 + 2 S_{T_e} \tau} \quad (25)$$

Note that the expression (25) satisfies Equation (18) if:

$$\int_1^{\lambda} \theta r dr = 0 \quad (26)$$

Equation (26) is merely a restatement of the assumption that the change in internal energy of the salt is negligible which will later be shown to be quite accurate for the system being considered.

#### Numerical Solution

The analytical solution derived above for the axisymmetric system is an accurate solution where the heat of fusion is numerically much larger than the specific heat of the storage material. If, however, the latent heat is not significantly larger numerically than the specific heat, then the assumption made to obtain that solution may be too strong to yield realistic results. For this reason a numerical solution in which the internal energy of the salt was accounted for was derived and is presented here.

Let the temperature distribution at time  $t^k$  be known in the form of

$$\theta_i^k = \theta(r_i, t^k) ; \quad 1 \leq i \leq n \quad (27)$$

Then if  $\lambda_{k+1} = \lambda(t^{k+1})$  is known we may find  $\theta_i^{k+1} \quad 1 \leq i \leq n+1$  from the tridiagonal matrix equation derived in Appendix A which is of the form

$$\begin{bmatrix} a_1 & b_1 & & & \\ c_2 & a_2 & b_2 & & \\ & c_3 & a_3 & b_3 & \\ & & & \ddots & \\ & & & & c_n & a_n \end{bmatrix} \begin{bmatrix} \theta_1 \\ \theta_2 \\ \theta_3 \\ \vdots \\ \theta_n \end{bmatrix} = \begin{bmatrix} d_1 \\ d_2 \\ d_3 \\ \vdots \\ d_n \end{bmatrix} \quad (28)$$

The procedure to calculate the temperature distribution is illustrated by the flow chart in Figure 3. First, a time increment  $\Delta\tau$  is selected and  $r(2)$  is calculated from Equation (25) as:

$$r(2) = \lambda_1 = \lambda(\Delta\tau) = \sqrt{1+2S_{Te}\Delta\tau} \quad (29)$$

and

$$\theta_1^1 = \theta(r=1) = \theta(r(1)) = \lambda \ln\left(\frac{1}{r(2)}\right) \quad (30)$$

and

$$\theta_2^1 = 0 \quad (31)$$

where the  $\theta$ 's are found from Equation (23).

From this point on, the procedure to find  $\theta_i^{k+1} = \theta_i^k$  is the same for each time step. Initially, it is assumed that  $\theta_i^{k+1} = \theta_i^k$  and  $\lambda_{k+1}$  is calculated from Equation (18) where

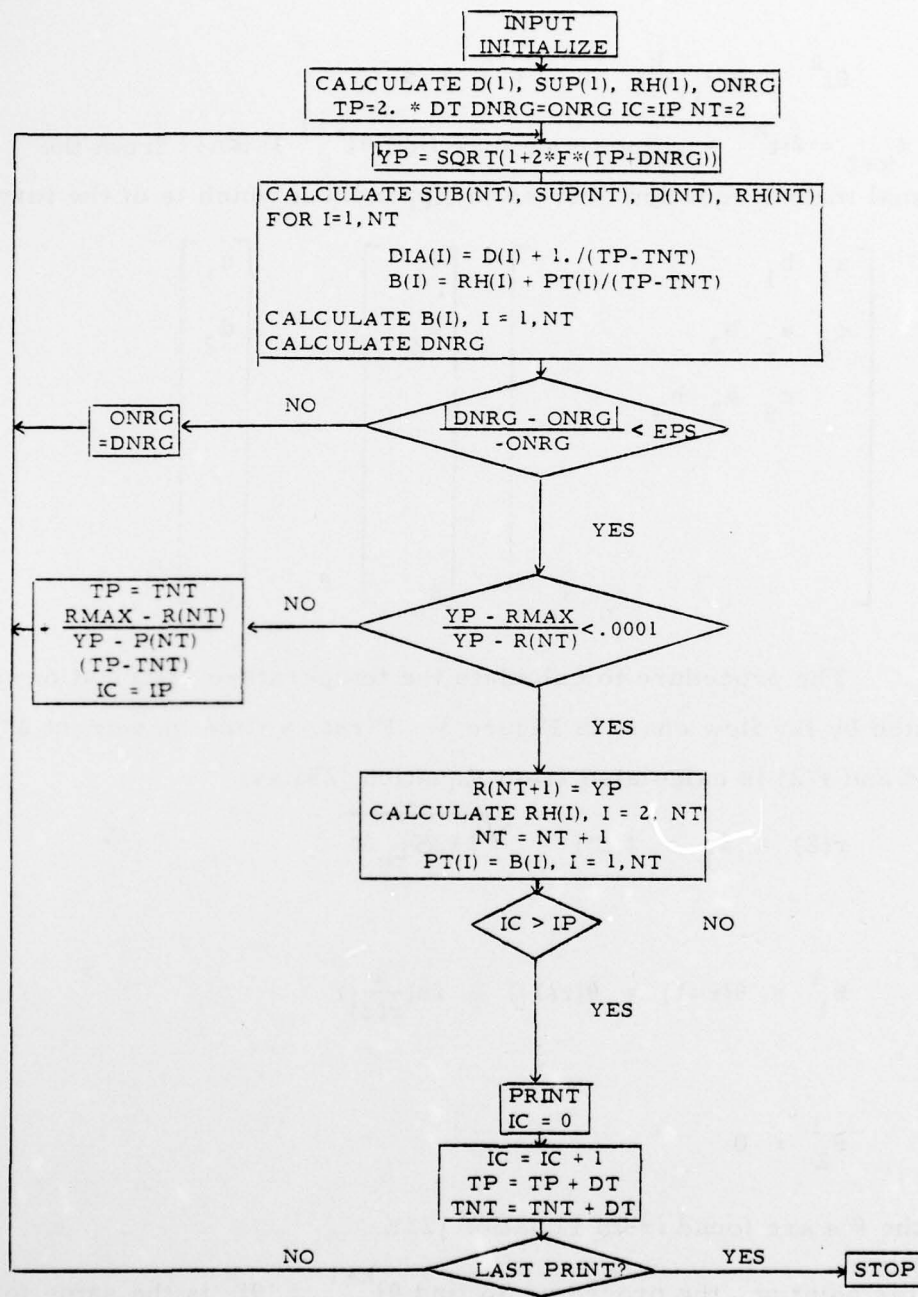


Figure 3. Flow Chart of Temperature Model of Axisymmetric HP/TES System

$$\int_1^L \theta_r dr = \sum_{i=2}^n \{(\theta_i^{k+1} r_i + \theta_{i-1}^{k+1} r_{i-1})/2\} (r_i - r_{i-1}) + \theta_n^{k+1} r_n (r_{n+1} - r_n)/2. \quad (32)$$

then  $\theta_i^{k+1}$ ,  $i=1, n$  are calculated from Equations (28). This temperature distribution is used to calculate a new  $\ell$  which in turn is used to calculate a new temperature distribution. This iterative procedure is continued until the change in  $\ell$  meets an acceptable error criteria at which point the temperature distribution for the new time has been calculated, and the procedure is initiated for the next time. The time increment is held uniform except that for the final time step,  $\Delta t$  is shortened so that  $\ell(\tau_f) = \ell_f$  from Equation (20). The computer program developed to calculate the axisymmetric temperature distribution is documented in Appendix B.

## SECTION VI

### ANALYSIS OF FINNED SYSTEM

#### Formulation of Equations

An approach similar to that used for the axisymmetric case could be used to model the finned system. However, the boundary would be much more difficult to locate since its location varies with the angle from the fin centerline. Instead an approach involving both the enthalpy and the temperature of the salt employed by Shamsunder and Sparrow<sup>(6)</sup> is used. In this approach, the solid liquid boundary is found as one of the results of the solution.

Since there was some uncertainty as to the accuracy of this method the method was first applied to the axisymmetric case and the results were used to examine the accuracy of the method. This formulation will be presented as an aid to understanding the approach. Then the method will be used to formulate the finned problem.

In this approach the region of interest is again divided into elements of finite size. If there are no sources of energy inside the control volume, pressure does not vary with time, and no external work is done on the control volume the net rate of increase of internal energy must equal the rate at which heat is conducted into the control volume. Then enthalpy and temperature are related in the law of conservation of energy for the element.

$$\frac{d}{dt} \iiint_v \rho h dv = \int_A k \text{grad } T \cdot \hat{n} dA \quad (33)$$

where  $h$  = specific enthalpy BTU/lbm

$\hat{n}$  = unit vector normal to the surface and directed outward from the control volume.

This may also be written in terms of dimensionless variables

$$\eta = \frac{1}{\rho \Delta v} \iiint_V \frac{\rho(h-h_f^*)}{hs\ell} dv \equiv \text{dimensionless enthalpy} \quad (34)$$

$$\theta = \frac{k_f(T-T^*)}{\alpha_f \rho h s \ell} \equiv \text{dimensionless temperature} \quad (35)$$

and enthalpy may be related to temperature by

$$h-h_f^* = \begin{cases} c(T-T_F) , & T < T_F \\ c(T-T_F)+hs\ell , & T > T_F \end{cases} \quad (36)$$

#### Axisymmetric Formulation and Solution

Let the region  $R_I < R < R_0$  be divided into  $n$  elements, each a concentric ring of width  $\Delta R$ . Let the thickness of the cannister wall be  $n_f \Delta R$ . Then, initially  $T = T_F$  and the thermal storage material is all liquid so that initially

$$\begin{aligned} \theta &= 0. & i &= 1, m \\ \eta &= 0. & i &\leq n_f \\ \eta &= 1. & n_f &< i \leq m \end{aligned} \quad (37)$$

where  $m = n + n_f$  total number of nodes.

Writing (33) in terms of the elements gives

$$\begin{aligned} p_n &= 2\pi R \Delta R h s \ell \frac{d}{dt} \frac{1}{\rho} \frac{1}{2\pi R \Delta R} \int_{R-\frac{\Delta R}{2}}^{R+\frac{\Delta R}{2}} \frac{\rho(h-h_f^*)}{h s \ell} dR \\ &- k_1 \frac{\partial T}{\partial r} 2\pi(R+\frac{\Delta R}{2}) - k_2 \frac{\partial T}{\partial r} 2\pi(R-\frac{\Delta R}{2}) \\ &- (k_1 \frac{\partial (k_n(T-T^*)/\alpha h s \ell)}{\partial R} 2\pi(R+\frac{\Delta R}{2}) - k_2 \frac{\partial (k_n(T-T^*)/\alpha h s \ell)}{\partial R} 2\pi(R-\frac{\Delta R}{2})) \frac{\alpha \rho s \ln \ell}{k_n} \end{aligned} \quad (38)$$

where  $k_1$  = thermal conductivity at outer edge of element

$k_2$  = thermal conductivity at inner edge of element.

Expressing (38) in terms of the dimensionless variables  $r$ ,  $\tau$ ,  $\theta$ , and  $\eta$  yields

$$\Delta r \frac{d\eta}{d\tau} = (1 + \frac{\Delta r}{2r_i}) \frac{k_1}{k_s} \frac{\partial \theta}{\partial r} \Big|_{r=r_i + \frac{\Delta r}{2}} - (1 - \frac{\Delta r}{2r_i}) \frac{k_2}{k_s} \frac{\partial \theta}{\partial r} \Big|_{r=r_i - \frac{\Delta r}{2}}$$

which can be expressed in terms of finite differences

$$\begin{aligned} \frac{(\Delta r)^2}{\Delta \tau} (\eta_i^k - \eta_i^{k-1}) &= (1 + \frac{\Delta r}{2r_i}) \frac{k_1}{k_s} (\theta_{i+1}^k - \theta_i^k) \\ &- (1 - \frac{\Delta r}{2r_i}) \frac{k_2}{k_s} (\theta_i^k - \theta_{i-1}^k) \end{aligned} \quad (39)$$

If the element is considered to be at a uniform temperature, substitute Equation (36) into (34) to find the relation between temperature and enthalpy:

$$\begin{aligned} \eta &= \frac{1}{\rho_s \Delta v} \int_{r_i - \frac{\Delta r}{2}}^{r_i + \frac{\Delta r}{2}} \frac{\rho c (T - T^*)}{h_{s,\ell}} dr \\ &= \frac{\rho c}{\Delta v} \frac{\alpha_s}{k_s} \frac{k_s (T - T^*)}{\alpha_s \rho_s h_{s,\ell}} \Delta v = \frac{\alpha_s k}{\alpha k_s} \theta \\ \theta &= \frac{\alpha k}{\alpha k_s} \eta \quad \eta < 0 \\ &= 0 \quad \eta > 0 \end{aligned} \quad (40)$$

Now, rearranging Equation (39) yields

$$\begin{aligned} \frac{(\Delta r)^2}{\Delta \tau} \eta_i^k + \left\{ (1 + \frac{\Delta r}{2r_i}) \frac{k_1}{k_s} + (1 - \frac{\Delta r}{2r_i}) \frac{k_2}{k_s} \right\} \theta_i^k \\ = \frac{(\Delta r)^2}{\Delta \tau} \eta_i^{k-1} + (1 + \frac{\Delta r}{2r_i}) \frac{k_1}{k_s} \theta_{i+1}^k + (1 - \frac{\Delta r}{2r_i}) \frac{k_2}{k_s} \theta_{i-1}^k ; \quad i = 2, \dots, m \end{aligned} \quad (41)$$

$$\text{where } k_1 = \begin{cases} k_f & h < h_f \\ 2 k_f k_s / (k_f + k_s) & h = h_f \\ k_s & h > h_f \end{cases}$$

$$k_2 = \begin{cases} k_f & h \leq h_f \\ 2 k_f k_s / (k_f + k_s) & h = h_f + 1 \\ k_s & h > h_f + 1 \end{cases}$$

Substitute for  $\theta$  from Equation (40) into the left hand side of Equation (41) to obtain

$$\left[ \frac{(\Delta r)^2}{\Delta \tau} + \frac{\alpha k_s}{\alpha_s k} \left[ \left( 1 + \frac{\Delta r}{2r_i} \right) \frac{k_1}{k_s} + \left( 1 - \frac{\Delta r}{2r_i} \right) \frac{k_2}{k_s} \right] \right] \eta_i^k$$

$$= \frac{(\Delta r)^2}{\Delta \tau} \eta_i^{k-1} + \left( 1 + \frac{\Delta r}{2r_i} \right) \frac{k_1}{k_s} \theta_{i+1}^k + \left( 1 - \frac{\Delta r}{2r_i} \right) \frac{k_2}{k_s} \theta_{i-1}^k , \quad \eta_i^k < 0 \quad (42)$$

and

$$\frac{(\Delta r)^2}{\Delta \tau} \eta_i^k = \frac{(\Delta r)^2}{\Delta \tau} \eta_i^{k-1} + \left( 1 + \frac{\Delta r}{2r_i} \right) \frac{k_1}{k_s} \theta_{i+1}^k + \left( 1 - \frac{\Delta r}{2r_i} \right) \frac{k_2}{k_s} \theta_{i-1}^k , \quad \eta_i^k > 0$$

At the inner surface of the innermost node, the heat flux is known so that Equation (33) may be written

$$\frac{\rho_s 2\pi R \Delta R h_{s\ell} \alpha_s}{R_I^2} \frac{d\eta}{d\tau} = \frac{k_1}{k_s} \frac{\partial \theta}{\partial R} 2\pi(R + \frac{\Delta R}{2}) \alpha_s \rho_s h_{s\ell} - 2\pi \dot{q}'' R_I$$

$$\text{where } \dot{q}'' = \frac{\dot{q}'}{2\pi R_I}$$

$$\frac{(\Delta r)^2}{\Delta \tau} (\eta_1^k - \eta_1^{k-1}) = \frac{k_1}{k_s} \left( 1 + \frac{\Delta r}{2r_1} \right) (\theta_2^k - \theta_1^k) - \frac{\dot{q}'' R_I}{\alpha_s \rho_s h_{s\ell}} \Delta r \quad (43)$$

Notice that the parameter  $S_{T_e}$  has again appeared on the right hand side of Equation (43). Since, in the previous analysis we concluded that this was the driving parameter for the solution, it is logical it should also appear in this formulation. Equation (43) may be rearranged similar to Equation (42) to yield

$$\left\{ \frac{(\Delta r)^2}{\Delta \tau} + \frac{\alpha k_s}{\alpha_s k} \left(1 + \frac{\Delta r}{2r_i}\right) \frac{k_1}{k_s} \right\} \eta_1^k = \frac{(\Delta r)^2}{\Delta \tau} \eta_1^{k-1} + \frac{k_1}{k_s} \left(1 + \frac{\Delta r}{2r_i}\right) \frac{\alpha k_s}{k \alpha_s} \theta_{i+1}^k - S T_e \Delta r$$

If  $\eta_1^k < 0$

(44)

Equations (42) and (44) are solved by Gauss-Seidel iteration with over-relaxation. The procedure is to first calculate the right hand side. Since the coefficient of  $\eta_i^k$  is always positive the sign of the right hand side is the same as that of  $\eta$  so that the appropriate coefficient may be determined.  $\eta$  is then calculated by dividing the right hand side by the coefficient of  $\eta$ . When the temperature distribution has been found with sufficient accuracy the volume solidified and the change in internal energy are calculated from:

$$V_s = \sum_{i=1}^m 2\pi r_i (\eta_i^0 - \max(\eta_i^k, 0.))$$
(45)

$$E_t = \sum_{i=1}^m 2\pi r_i (\eta_i^0 - \eta_i^k)$$
(46)

#### Finned System Formulation and Solution

The model for the finned system is set up very similarly to that for the axisymmetric system. Since the temperature may vary with angle as well as radius two spatial dimensions must be included in the model. Because of the symmetry assumed, only the shaded region in Figure 2 need be modeled and the heat flux across the boundaries  $\psi = 0$  and  $\psi = \pi/(\text{no. of fins})$  is known to be zero. Also because heat losses are neglected there is no heat flux across the outer surface. The heat flux across the inner boundary is specified as part of the problem so that the heat flux is known over the entire boundary of the region.

We write the enthalpy equation for an element containing a volume  $f\Delta v$  of fin material and a volume  $(1-f)\Delta v$  of salt and having thermal conductivities  $k_1$ ,  $k_2$ ,  $k_3$ , and  $k_4$  on the surfaces  $r = r_i + \frac{\Delta r}{2}$ ,  $\psi = \psi_i + \frac{\Delta \psi}{2}$ ,

$r = r_i - \frac{\Delta r}{2}$ , and  $\psi = \psi_i - \frac{\Delta \psi}{2}$  respectively. Then Equation (33) may be written

$$\begin{aligned} \frac{(\Delta r)^2}{\Delta \tau} \eta_{i,j}^k + & \left[ \left(1 + \frac{\Delta r}{2r}\right) \frac{k_1}{k_n} + \frac{k_2}{k_n} \left(\frac{\Delta r}{r \Delta \tau}\right)^2 + \left(1 - \frac{\Delta r}{2r}\right) \frac{k_3}{k_n} + \frac{k_4}{k_n} \left(\frac{\Delta r}{r \Delta \tau}\right)^2 \right] \theta_{i,j}^k \\ & - \frac{(\Delta r)^2}{\Delta \tau} \eta_{i,j}^{k-1} + \left(1 + \frac{\Delta r}{2r}\right) \frac{k_1}{k_n} \theta_{i+1,j}^k + \frac{k_2}{k_n} \left(\frac{\Delta r}{r \Delta \tau}\right)^2 \theta_{i,j+1}^k \\ & + \left(1 - \frac{\Delta r}{2r}\right) \frac{k_3}{k_n} \theta_{i-1,j}^k + \frac{k_4}{k_n} \left(\frac{\Delta r}{r \Delta \tau}\right)^2 \theta_{i,j-1}^k \end{aligned} \quad (47)$$

Now we use Equation (34) to establish the relation between  $\eta$  and  $\theta$  assuming the element at uniform temperature

$$\begin{aligned} \eta &= \frac{1}{\rho_s \Delta v} \iiint \frac{\rho(h-h_s)}{h_s \ell} dv \\ &= \frac{\rho c_f (T - T_s^*)}{\rho_s \Delta v h_s \ell} f \Delta v + \frac{\rho_s c_s}{\rho_s \Delta v} \frac{T - T_s^*}{h_s \ell} (1-f) \Delta v \\ &= \frac{k_s (T - T_s^*)}{\alpha_s \rho_s h_s \ell} \{ f \frac{\alpha_s}{k_s} \rho_f c_f + (1-f) \} \\ \theta &= \begin{cases} \frac{\eta}{1 - f(1 - \frac{\alpha_s k_f}{k_s \alpha_f})}, & \eta < 0 \\ 0, & 0 < \eta < 1. \end{cases} \end{aligned} \quad (48)$$

Equation (47) must be modified for boundary elements similar to the axisymmetric case. The iterative procedure for solution is illustrated by the flow chart in Figure 4. Here, Equation (47) is expressed:

$$\begin{aligned} \eta_{i,j}^k &= [D \eta_{i,y}^{k-1} + C1(I, J) \cdot \eta_{i+1,j}^k + C2(I, J) \cdot \eta_{i,j+1}^k + C3(I, J) \cdot \eta_{i-1,j}^k \\ &+ C4(I, J) \cdot \eta_{i,j-1}^k] / C5(I, J) \\ C5(I, J) &= D + (C1(I, J) + C2(I, J) + C3(I, J) + C4(I, J)) / \left(1 - \frac{\alpha_s k_f}{\alpha_f k_s}\right) \end{aligned} \quad (49)$$

when  $\eta_{i,j}^k = 0$ .

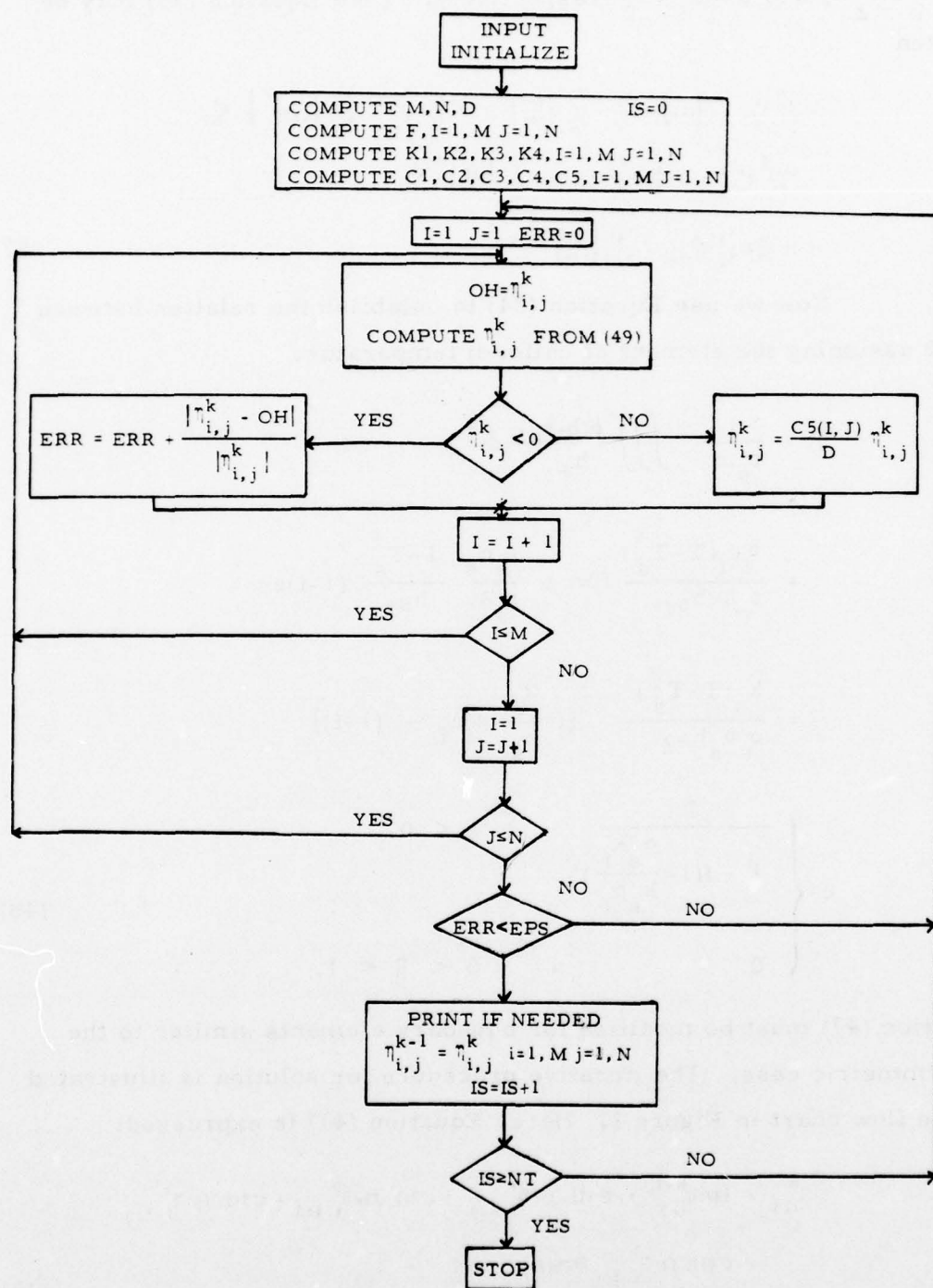


Figure 4. Flow Chart for Enthalpy Model of Finned HP/TES System

SECTION VII  
RESULTS AND DISCUSSION

Results with Axisymmetric Case

The approximate analytical solution as previously derived in dimensionless form is

$$\theta = \ln(r/\ell) \quad (23)$$

$$\ell = \sqrt{1 + 2ST_e \tau} \quad (25)$$

If this solution is correct, the change in energy from the heat fusion is

$$\pi R_I^2 (\ell^2 - 1) \rho h_s \ell = \Delta E.$$

and the change in internal energy of the salt, which was neglected is

$$\begin{aligned} \Delta E_2 &= \int_{R_I}^{R_0} \frac{k}{\alpha} (T - T_F) 2\pi R dR \\ &= \int_1^{\ell} \frac{2\pi \dot{q}'' R_I^3}{\alpha} \frac{k(T - T_F)}{q'' R_I} r dr \\ &= \frac{2\pi \dot{q}'' R_I^3}{\alpha} \int_1^{\ell} \theta r dr \end{aligned} \quad (50)$$

Substituting Equations (23) into (50) and integrating yields

$$\Delta E_2 = \frac{2\pi \dot{q}'' R_I^3 \ell^2}{\alpha} \left\{ \frac{1 - \ell^2}{4} + \frac{1}{2} \ln(\ell) \right\} \quad (51)$$

The ratio of the neglected energy change  $\Delta E_2$  to the change from the heat fusion  $\Delta E_1$  is

$$\begin{aligned}\frac{\Delta E_2}{\Delta E_1} &= \frac{q''R_I}{\alpha \rho h_s} \frac{\ell^2}{\ell^2 - 1} \ln(\ell) - \frac{1}{2} \\ &= S_{T_e} \frac{\ell^2}{\ell^2 - 1} \ln(\ell) - \frac{1}{2} \quad (52)\end{aligned}$$

In the worst case (heat rate = 1.5 kw,  $\ell = \ell_f$ ) the neglected heat is only 10.8% of the heat included so that the approximate solution is fairly accurate for the system. Since the change in internal energy of the solid salt is such a small part of the heat extracted from the system, the solidification times predicted by this simple model will be very accurate, even if part of the solidification takes place on the outer wall due to heat losses. In this case however, the temperature drop would be less than that predicted since the heat of fusion would not have to be conducted across as thick a layer of solidified salt.

Before meaningful results could be obtained for the numerical solutions for the axisymmetric case, it was necessary to determine convergence. In this program the increments in both radius and time are determined by the parameter  $\Delta t$  and was for each case half that of the preceding case. Once the temperatures agreed for consecutive time increments to three significant digits, convergence was assumed to be adequate. For the runs with other heat rates,  $\Delta t$  was adjusted to maintain the same increment in radius.

In Figure 5 temperature is plotted as a function of radius for several different times for the axisymmetric system with a heat extraction rate of 1 kw. Both the analytical and the numerical solutions are shown. It may be seen that at any given time the numerical solution predicts a slightly smaller interface radius than does the analytical

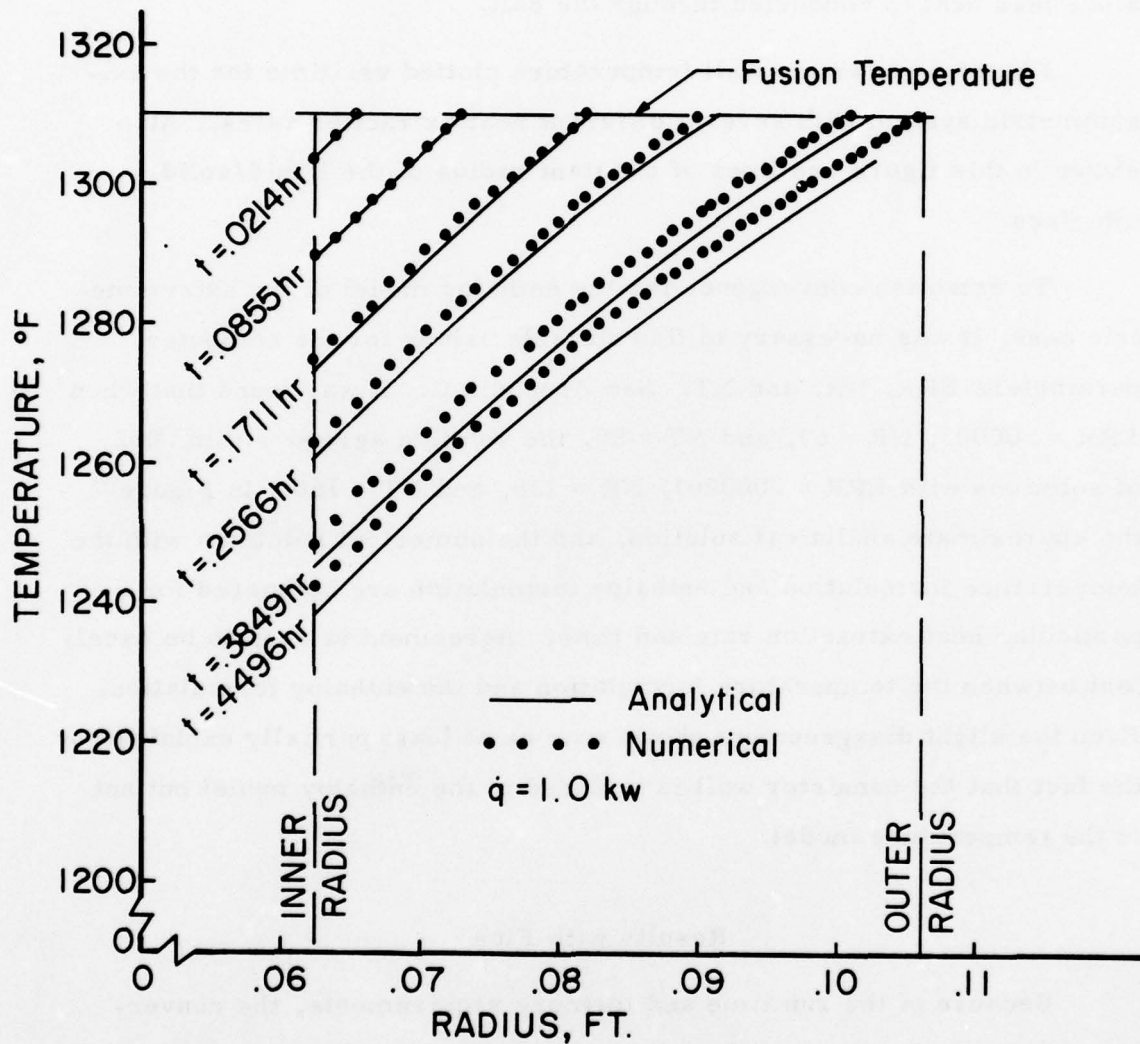


Figure 5. Temperature Distribution As A Function of Radial Position in HP/TES System (Axisymmetrical Case)

solution. This is because a small amount of the heat extracted comes from the change in internal energy of the solid salt. Therefore the salt solidifies more slowly than predicted by the analytical model to yield the heat which is extracted from the system. Also, the temperature gradient at the inner radius is less steep than predicted by the analytical model since less heat is conducted through the salt.

Figure 6 shows the wall temperature plotted vs. time for the axisymmetric system with several different heat extraction rates. Also shown in this figure are lines of constant radius of the liquid/solid interface.

To establish convergence for the enthalpy model of the axisymmetric case, it was necessary to find suitable values for the computer parameters ERR, NR, and NT. See Appendix C. It was found that when  $ERR = .00001$ ,  $NR = 63$ , and  $NT = 80$ , the solution agreed within .002 of solutions with  $ERR = .000001$ ,  $NR = 126$ , and  $NT = 160$ . In Figure 7 the approximate analytical solution, and the numerical solutions with the temperature formulation and enthalpy formulation are compared for a particular heat extraction rate and time. Agreement is seen to be excellent between the temperature formulation and the enthalpy formulation. Even the slight disagreement shown may be at least partially explained by the fact that the cannister wall is included in the enthalpy model but not in the temperature model.

#### Results with Fins

Because of the run time and memory requirements, the convergence criteria for the finned model was based on results with the axisymmetric model. The convergence study on the axisymmetric model showed that NT and ERR were most detrimental to accuracy. See Appendix D. Therefore the finned model cases were run with computer parameters  $NR = 21$ ,  $NS = 30$ ,  $NT = 80$ , and  $ERR = .00001$ .

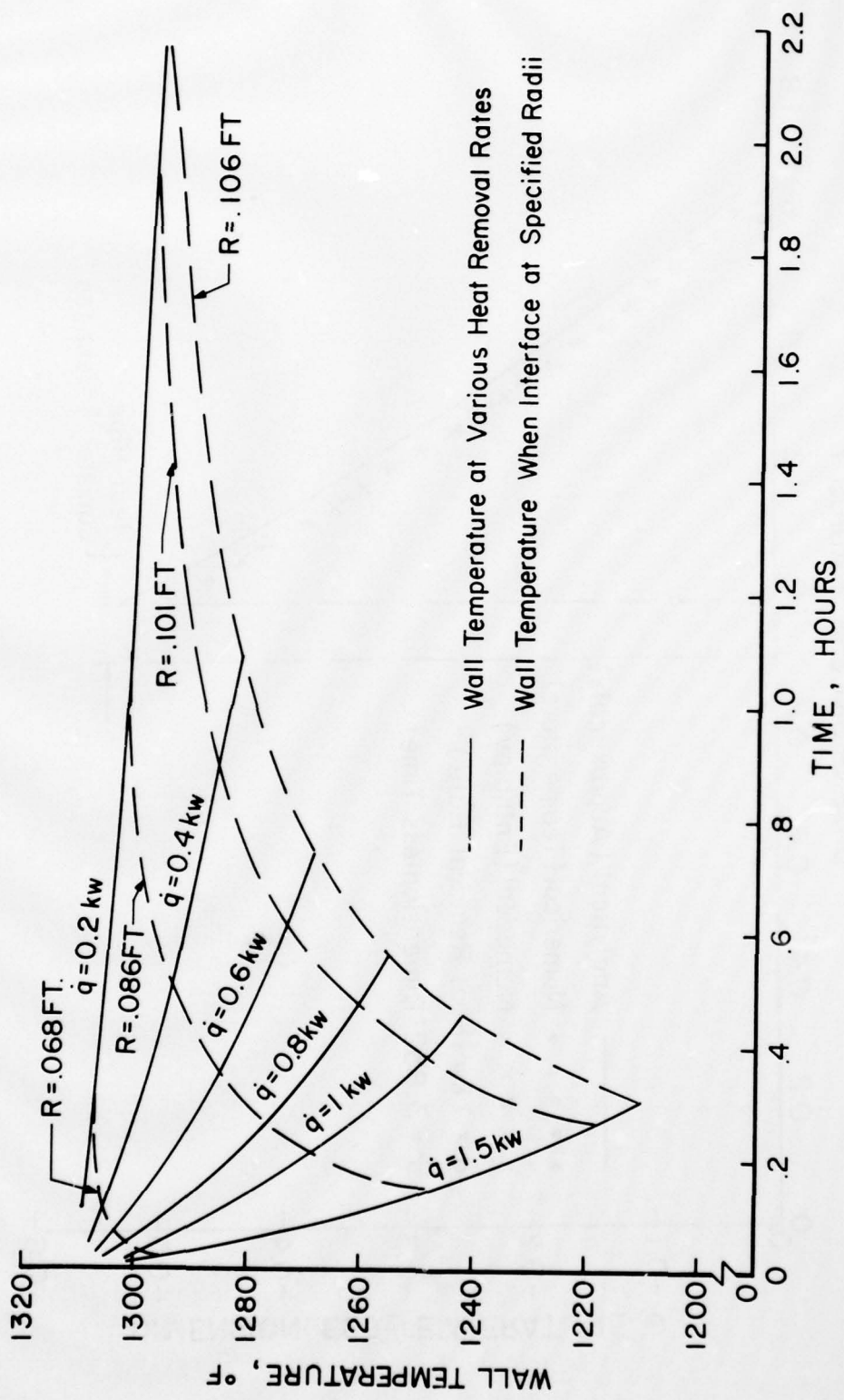


Figure 6. Wall Temperature and Interface Location in HP/TES System

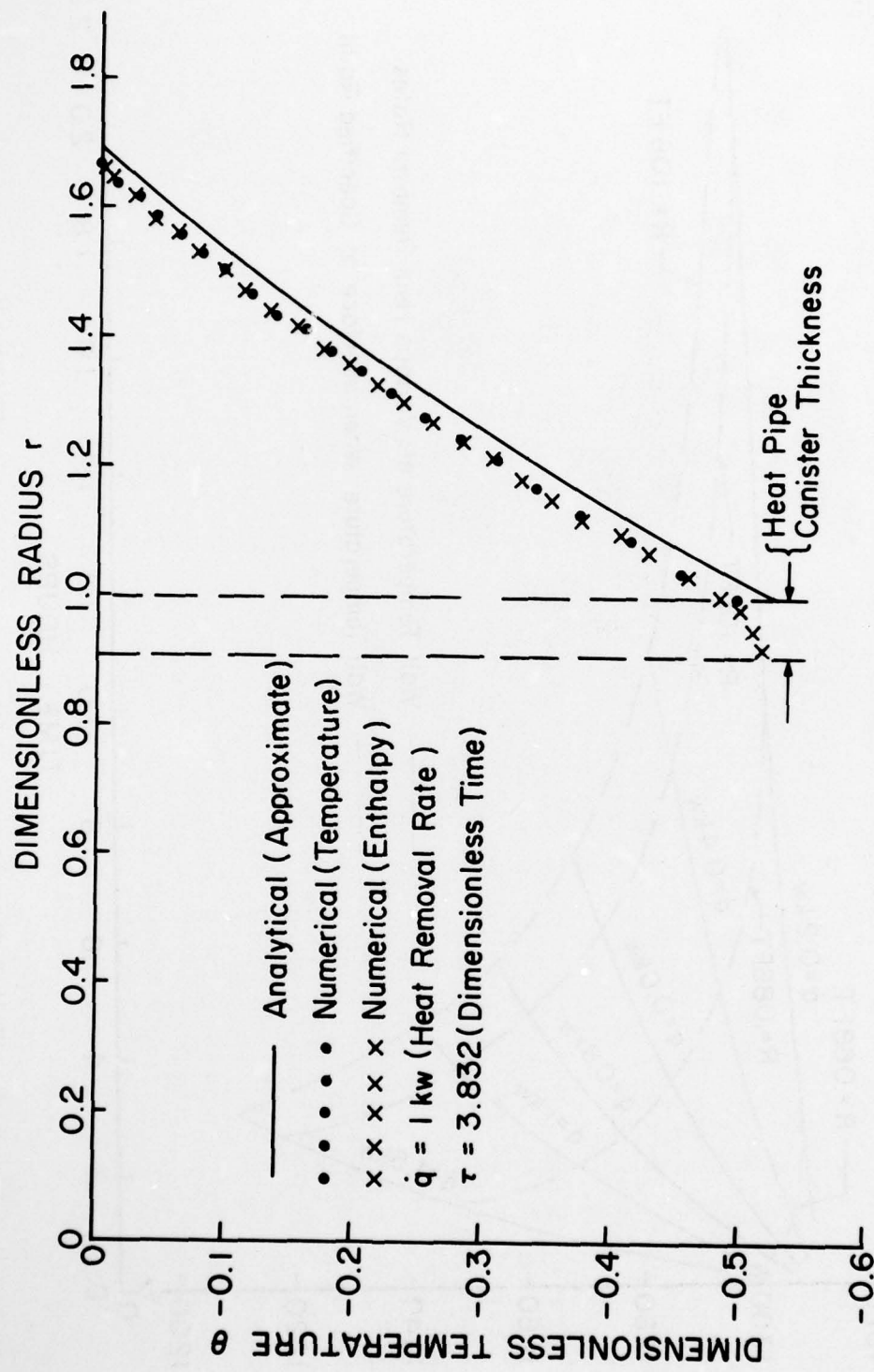


Figure 7. Temperature Distribution in Axisymmetric HP/TES System Determined Analytically and by Two Numerical Techniques

Figures 8, 10, 12, 14, and 16 show the interface radius plotted versus angle from the fin centerline for heat extraction rates of .25, .50, .75, 1.0, and 1.5 kw at several times. They show that a significant amount of freezing takes place along the fin but the close agreement of the interface shape for the two configurations indicates a similar amount of heat is extracted by the fins in each case. Figures 9, 11, 13, 15, and 17 show the wall temperature profiles for the same cases. Note that a significant reduction in the temperature drop is obtained with fins. This reduction is seen to increase with time and with heat extraction rate. It appears from the figures that most of the temperature drop obtained with 6 fins is also obtained with three fins.

Figure 18 shows the wall temperature as a function of the heat extracted for the zero, three and six fin configurations and a 1 kw heat rate. The effectiveness of fins as a device for reduction of total system weight was assessed in the following manner. The maximum allowable dimensionless temperature drop was arbitrarily selected to be 0.4. From Figure 18 the amount of heat extracted was as shown in column 2 of Table 2. The interface radius for the axisymmetric configuration was  $\ell = 1.513$  and with a 30% void volume allowance, the outer radius is  $r_o = 1.6857$  and the dimensionless volume is  $v = 1.8416$ . The other cases were sized to provide for the same volume of salt resulting in the outer radii shown in column 4 of the table. The lengths required to provide an equivalent amount of heat are shown in column 3 and the dimensionless system weights are shown in column 5. It may be seen that despite the shorter lengths for the finned configurations, the systems with fins are much heavier than the conventional configuration without fins. Thus the given fins are probably not an effective way to reduce the temperature drop when system weight is a prime consideration.

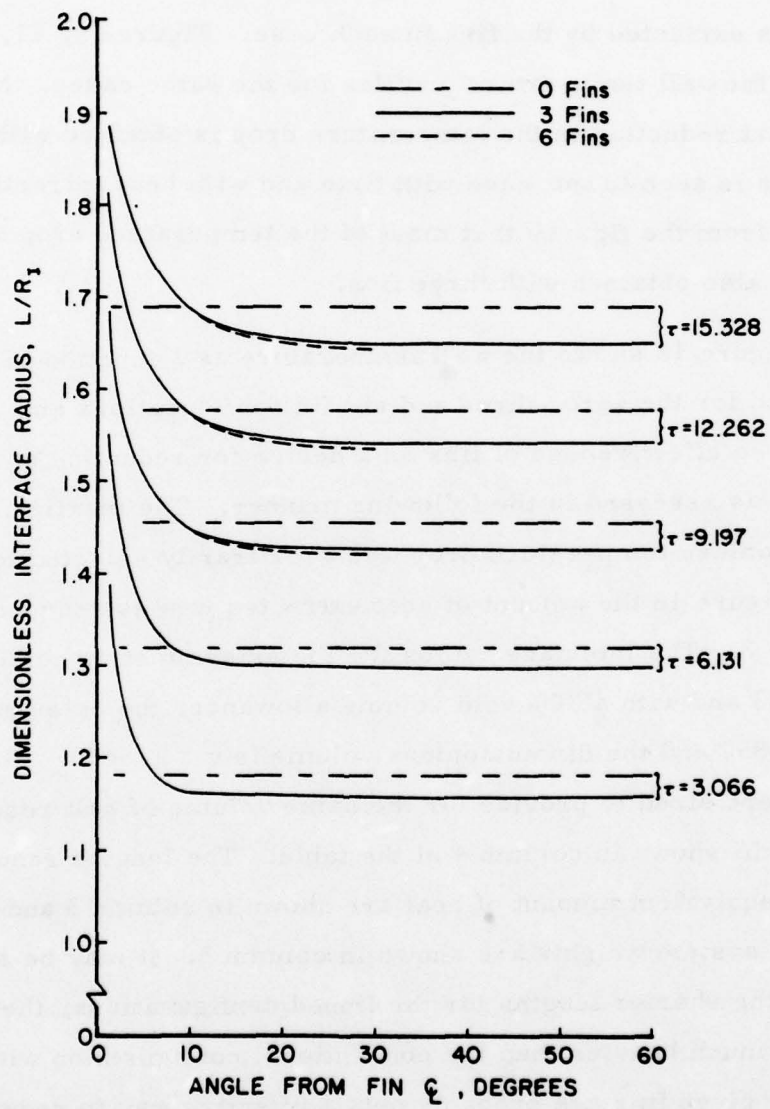


Figure 8. Interface Radius vs. Angle for 0, 3, & 6 Fin  
HP/TES Systems, Heat Extraction Rate = 0.25  
kw

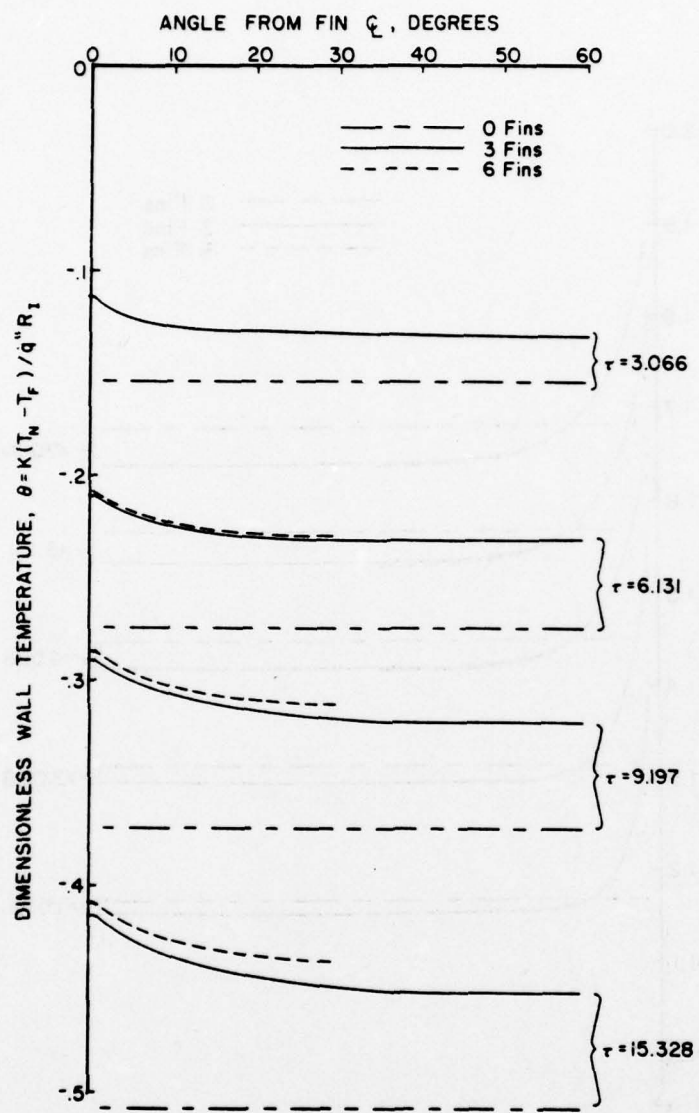


Figure 9. Wall Temperature vs. Angle for 0, 3, & 6 Fin HP/TES Systems, Heat Extraction Rate = 0.25 kw

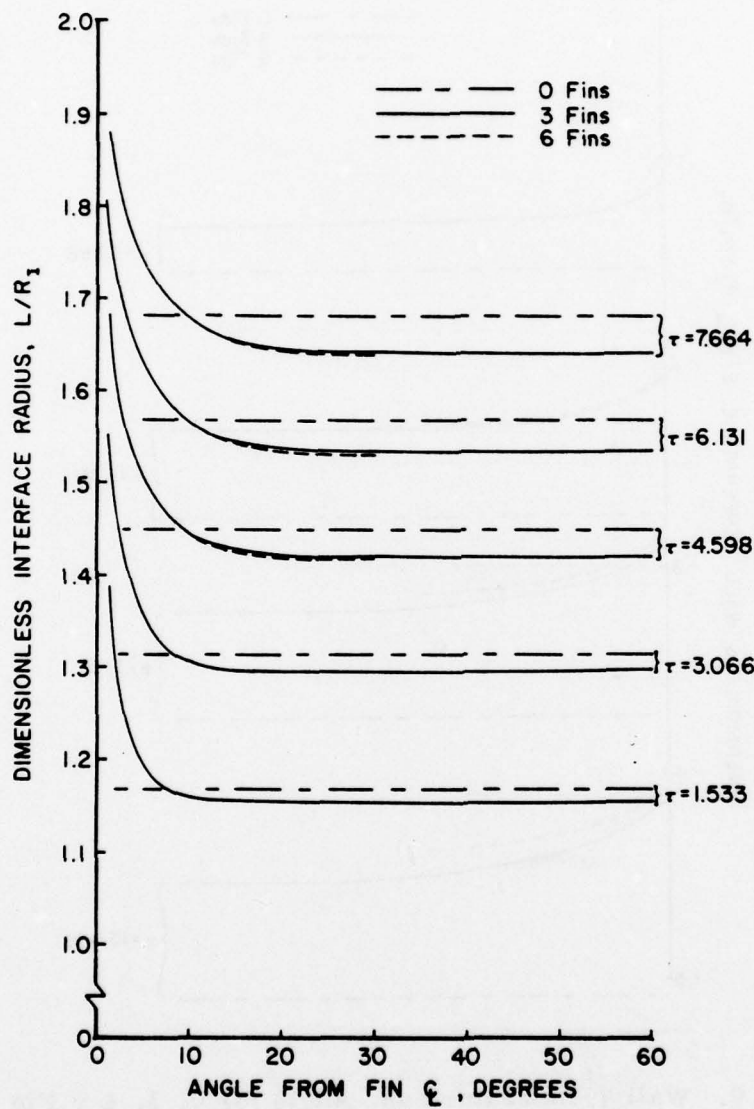


Figure 10. Interface Radius vs. Angle for 0, 3, & 6 Fin  
HP/TES Systems, Heat Extraction Rate = 0.50 kw

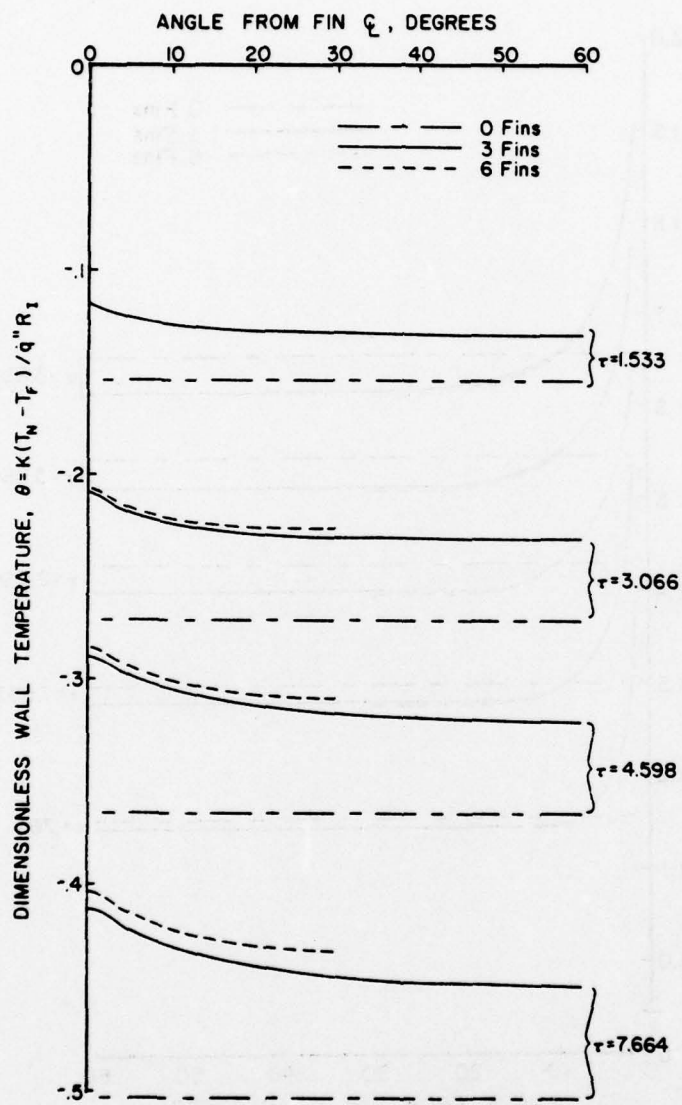


Figure 11. Wall Temperature vs. Angle for 0, 3, & 6 Fin HP/TES Systems, Heat Extraction Rate = 0.50 kw

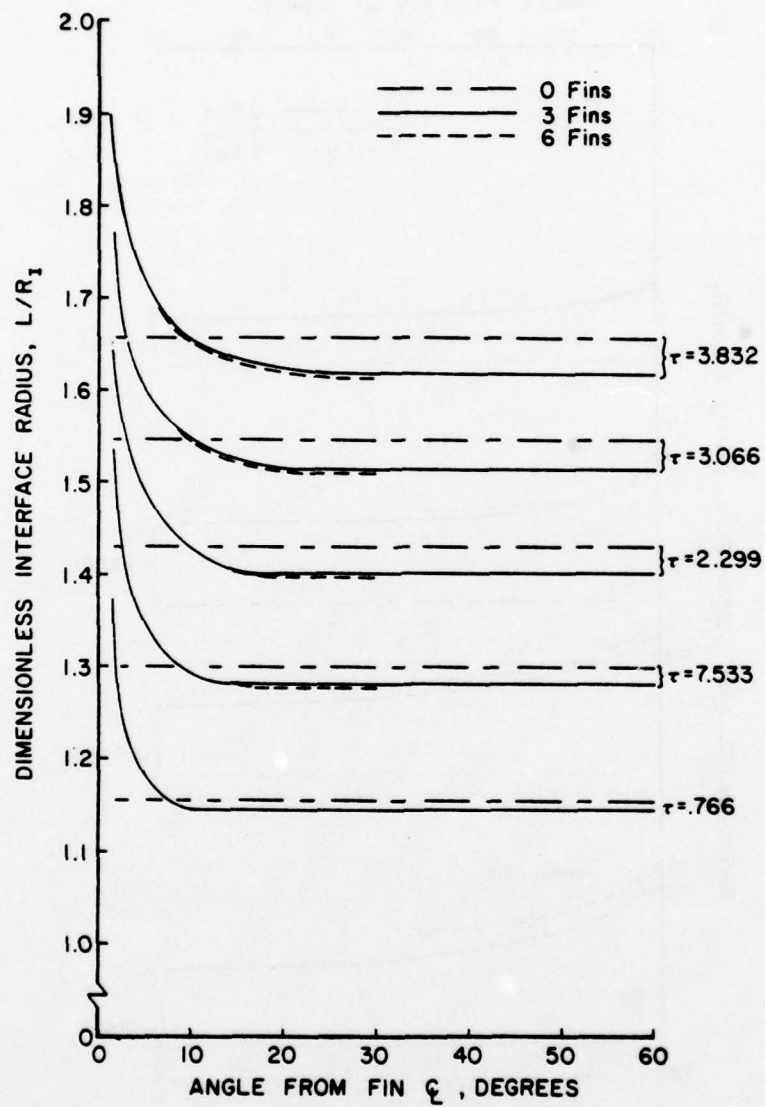


Figure 12. Interface Radius vs. Angle for 0 and 6 Fin HP/TES Units, Heat Extraction Rate = 0.75 kw

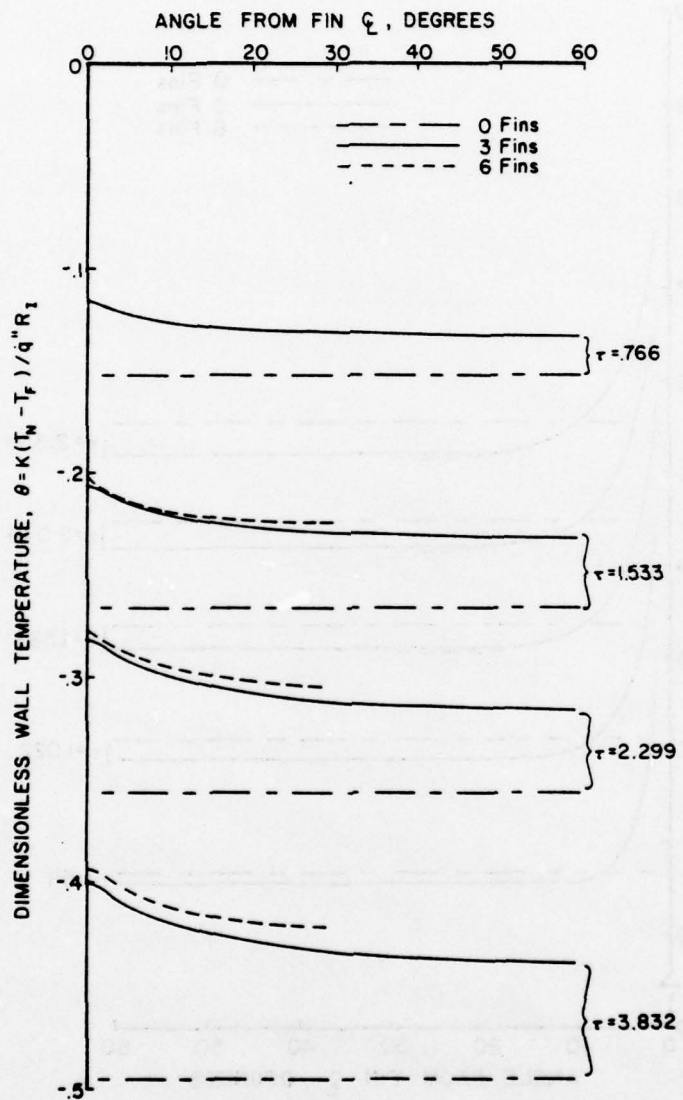


Figure 13. Wall Temperature vs. Angle for 0 and 6 Fin HP/TES Units, Heat Extraction Rate = 0.75 kw

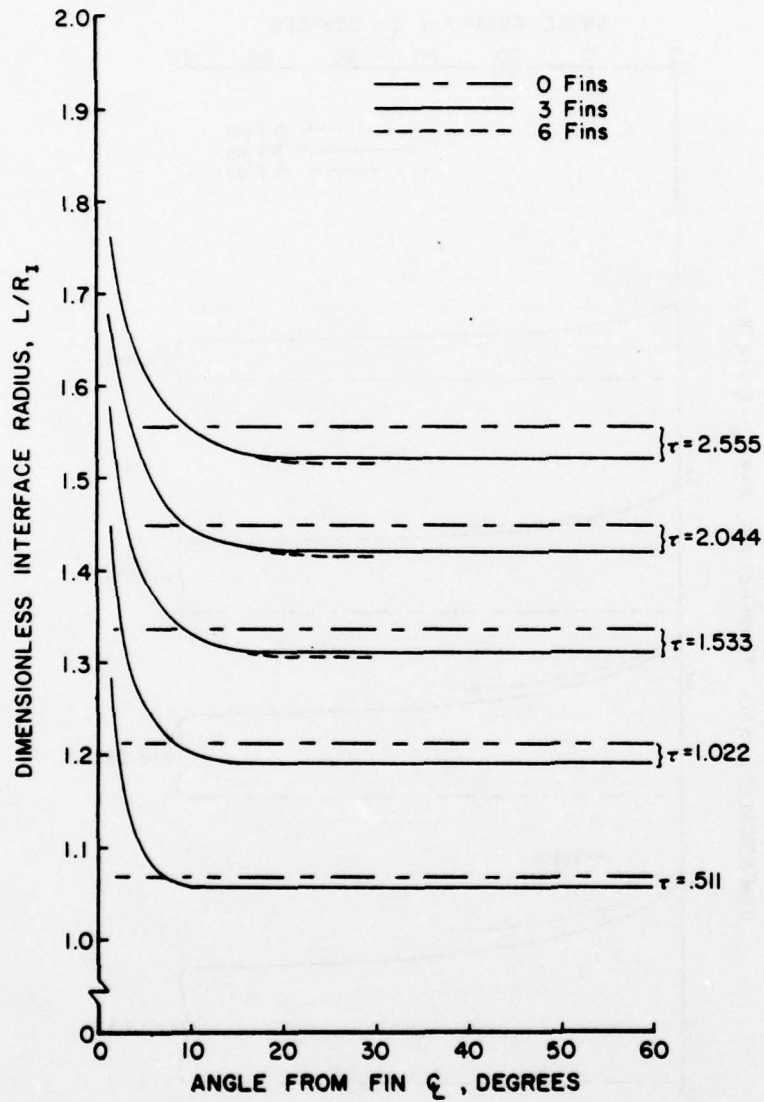


Figure 14. Interface Radius vs. Angle for 0, 3, & 6 Fin HP/TES Units, Heat Extraction Rate = 1.00 kw

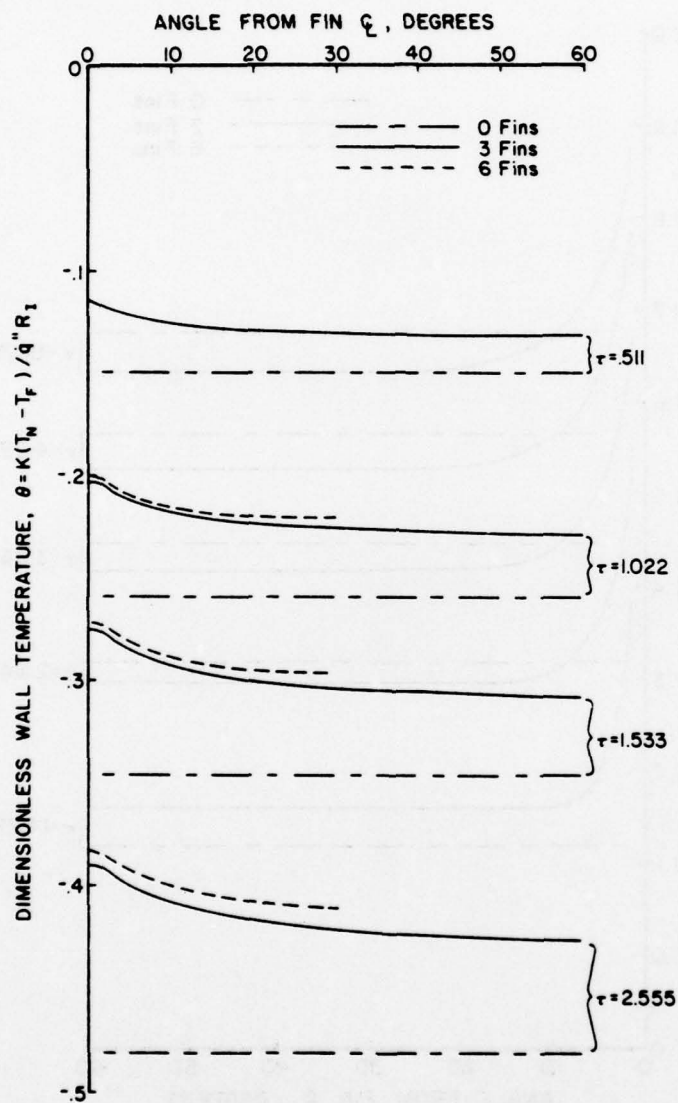


Figure 15. Wall Temperature vs. Angle for 0, 3, & 6 Fin HP/TES Units, Heat Extraction Rate = 1.00 kw

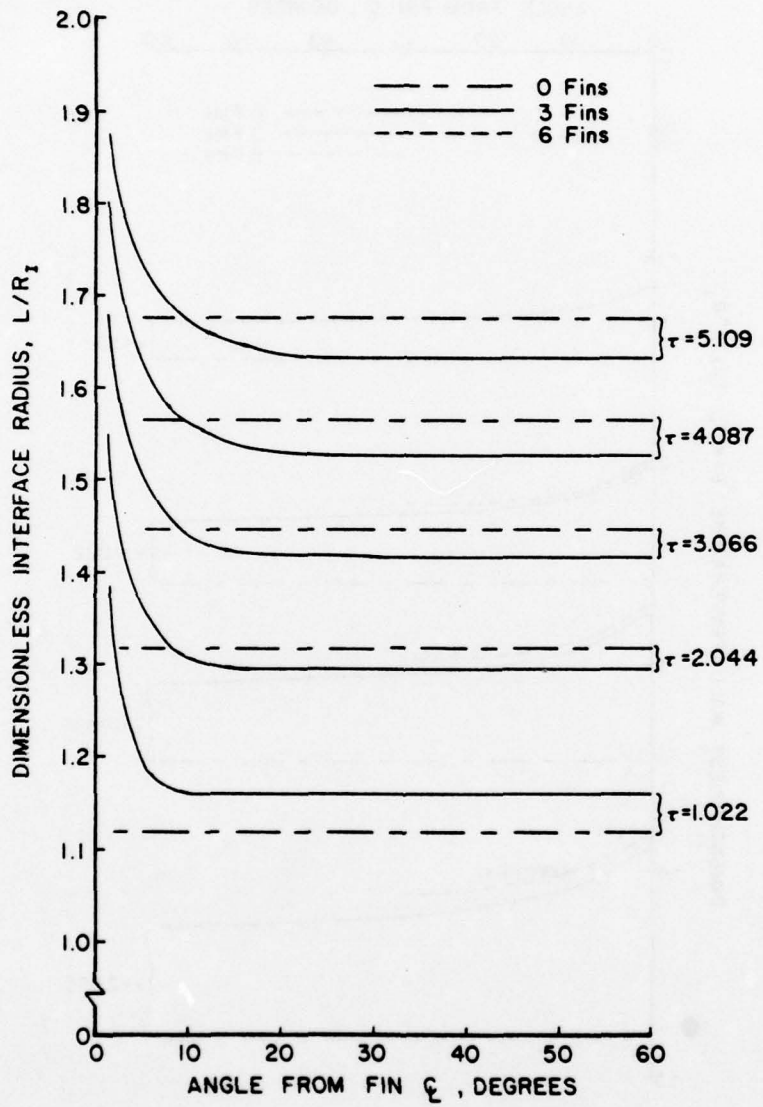


Figure 16. Interface Radius vs. Angle for 0, 3, & 6 Fin HP/TES Units, Heat Extraction Rate = 1.50 kw

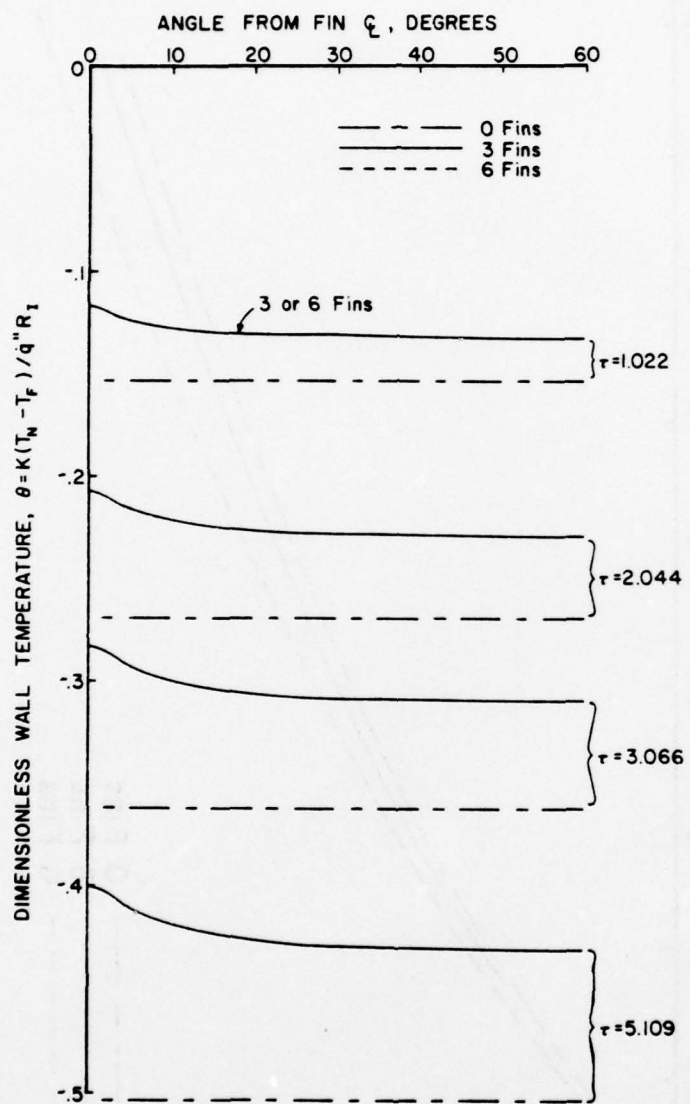


Figure 17. Wall Temperature vs. Angle for 0, 3, & 6 Fin HP/TES Units, Heat Extraction Rate = 1.50 kw

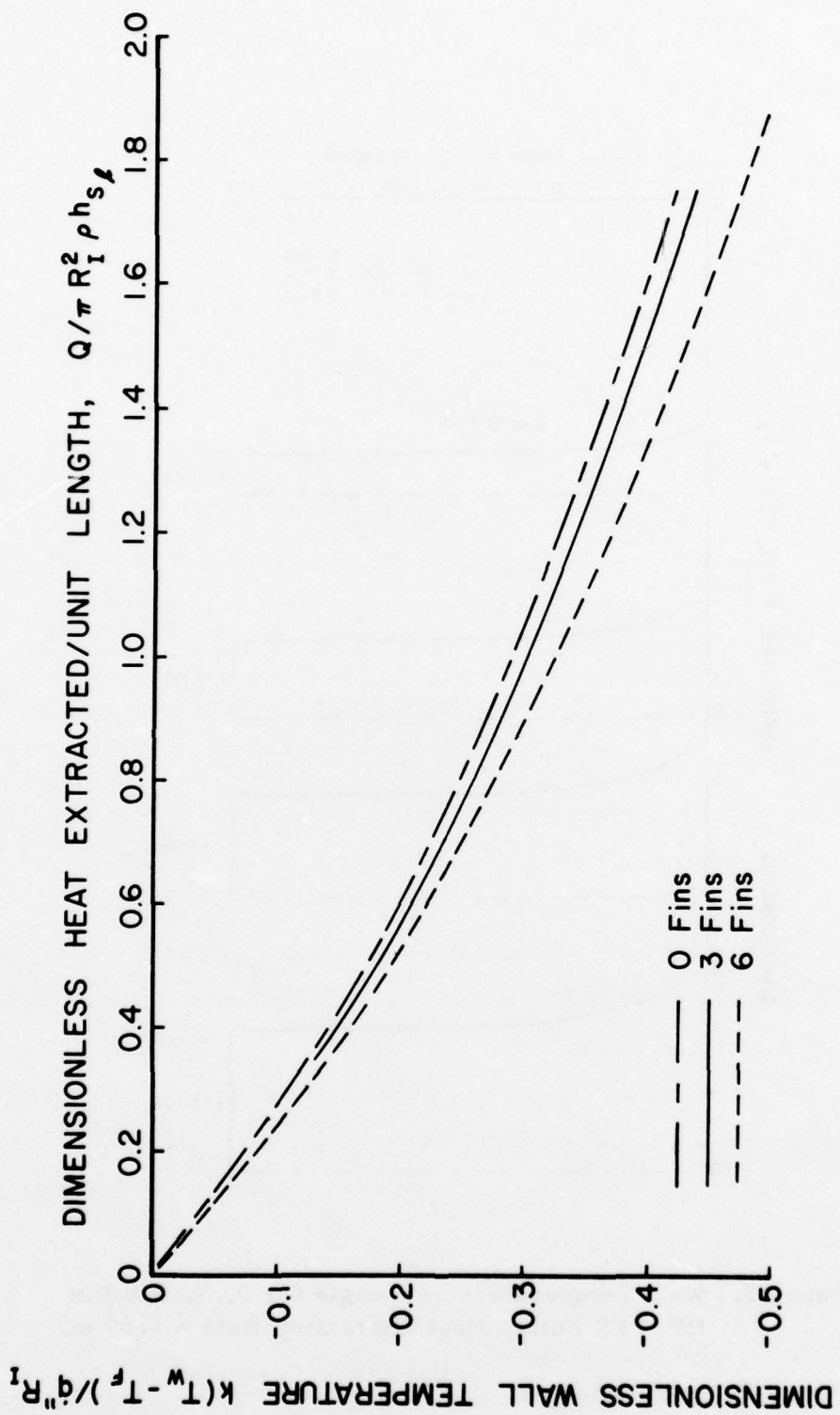


Figure 18. Heat Extracted vs. Wall Temperature for 0, 3, & 6 Fin HP/TES Units

TABLE 2  
FIN EFFECTIVENESS

Heat Extraction Rate = 1 kw  
Dimensionless Wall Temperature = -0.4

| No. of Fins | <u>Heat Extracted</u><br>Unit Length | Relative Length | $R_0/R_I$ | Relative Weight |
|-------------|--------------------------------------|-----------------|-----------|-----------------|
| 0           | 1.36                                 | 1.0             | 1.686     | 1.              |
| 3           | 1.52                                 | .8947           | 1.766     | 1.0387          |
| 6           | 1.62                                 | .8395           | 1.823     | 1.1189          |

## SECTION VIII

### SUMMARY AND CONCLUSIONS

The heat transfer process has been successfully modeled for both axisymmetric and finned systems. For axisymmetric systems the temperature formulation may be solved very quickly, providing a solution which is extremely accurate. The difficulty in locating the interface boundary makes it difficult to adapt this formulation to two dimensional systems.

For those systems, the enthalpy model provides a system in which the temperature distribution and interface boundary are found simultaneously. When this formulation was applied to the axisymmetric system it was found that accuracies were as good as those attained with the temperature model but that an order of magnitude greater computer time was required to obtain the solution.

For the finned system, an additional order of magnitude of computer time was required to obtain the solution. The solutions with fins are slightly less accurate than the axisymmetric since it wasn't practical to study convergence fully. Solutions were attained with sufficient accuracy, however, to give a meaningful comparison of the finned systems to the axisymmetric system. It was found that some reduction of the temperature drop at the inner wall was attained with fins but that systems employing fins would in turn be heavier. Thus fins may not be practical for this particular fin/system design.

## SECTION IX RECOMMENDATIONS

Although the analytical and numerical techniques developed were very accurate, the final solution may be adversely affected by the accuracy of the measured properties of the salts as well as the limiting assumptions used in deriving the governing equations. Based on the analysis completed it is recommended that

- 1) The salt physical properties, liquid and solid, should be accurately determined.
- 2) The effect of radiation to and from the salt, liquid and solid, should be assessed. Radiation properties of the salt are needed.
- 3) The experimental apparatus should be redesigned to (a) relieve hydrostatic stresses on melting, (b) improve calorimetry and (c) determine a fin configuration to optimize heat transfer.
- 4) The temperature model for the axisymmetric case may be useful to study boundary conditions which vary with time since it is solved so quickly. It is recommended that this program be suitably modified and studies of the effects of time varying heat extraction rate be conducted.
- 5) The enthalpy model has the versatility to study solidification fronts in unusual geometries. This model should be refined to shorten the solution time and better define the accuracy. It could then be used to examine other two dimensional configurations, including the axial variation of the nonfinned case and the assymmetry due to the volume void on solidification.
- 6) The model of the axisymmetric system should be expanded to include the heat transfer within the heat pipe and the calorimeter.

Such an expanded model would be useful in the design of further experiments with such systems.

## APPENDIX A

### AXISYMMETRIC HEAT CONDUCTION EQUATION

In this appendix the axisymmetric 1-Dimensional heat conduction equation in cylindrical coordinates is written in finite difference form for a variable mesh grid. This equation is:

$$\frac{\partial^2 \theta}{\partial r^2} + \frac{1}{r} \frac{\partial \theta}{\partial r} = \frac{\partial \theta}{\partial \tau} \quad (A.1)$$

Where  $\theta$  is the dimensionless temperature at time  $\tau$  and radius  $r$ . The object is to express Equation (A.1) at  $r = r_k$  in terms of the temperatures  $\theta_{k-1}$ ,  $\theta_k$  and  $\theta_{k+1}$  at radii  $r_{k-1}$ ,  $r_k$ , and  $r_{k+1}$  respectively. To do this write  $\theta_{k+1}$  and  $\theta_{k-1}$  by Taylor Series:

$$\begin{aligned} \theta_{k+1} &= \theta_k + (r_{k+1} - r_k) \frac{\partial \theta}{\partial r} + \frac{(r_{k+1} - r_k)^2}{2!} \frac{\partial^2 \theta}{\partial r^2} + \dots \\ \theta_{k-1} &= \theta_k - (r_k - r_{k-1}) \frac{\partial \theta}{\partial r} + \frac{(r_k - r_{k-1})^2}{2!} \frac{\partial^2 \theta}{\partial r^2} + \dots \end{aligned} \quad (A.2)$$

Neglect higher order terms and solve Equations (A.2) for  $\frac{\partial \theta}{\partial r}$  and  $\frac{\partial^2 \theta}{\partial r^2}$  to obtain

$$\begin{aligned} \frac{\partial \theta}{\partial r} &\approx \frac{(r_k - r_{k-1})^2 \theta_{k+1} + (-r_{k+1} + 2r_k - r_{k-1})(r_{k+1} - r_{k-1}) \theta_k - (r_{k+1} - r_k)^2 \theta_{k-1}}{(r_{k+1} - r_k)(r_k - r_{k-1})(r_{k+1} - r_{k-1})} \\ \frac{\partial^2 \theta}{\partial r^2} &\approx 2 \frac{(r_k - r_{k-1}) \theta_{k+1} - (r_{k+1} - r_{k-1}) \theta_k + (r_{k+1} - r_k) \theta_{k-1}}{(r_{k+1} - r_k)(r_k - r_{k-1})(r_{k+1} - r_{k-1})} \end{aligned} \quad (A.3)$$

Substitute Equation (A.3) into the right hand side of (A.1) and group terms to obtain:

$$\begin{aligned}
 \frac{\partial^2 \theta}{\partial r^2} + \frac{1}{r} \frac{\partial \theta}{\partial r} &= \frac{1}{r_k(r_{k+1}-r_{k-1})(r_{k+1}-r_k)(r_k-r_{k-1})} \\
 &\{(3r_k-r_{k+1})(r_{k+1}-r_k)\theta_{k-1} + (4r_k-r_{k+1}-r_{k-1})(r_{k+1}-r_{k-1})\theta_k \\
 &+ (3r_k-r_{k-1})(r_k-r_{k-1})\theta_{k+1}\} \\
 &= -2(c_k\theta_{k-1} + a_k\theta_k + b_k\theta_{k+1}) \quad (A.4)
 \end{aligned}$$

Let  $\theta$  represent the temperature at time  $\tau$  and  $\phi$  represent the temperature at an earlier time  $\tau - \Delta\tau$ . The right hand side of Equation (A.1) is written by finite differences and the Crank-Nicholson method is employed. Then:

$$\begin{aligned}
 \frac{1}{2} \left\{ \frac{\partial^2 \theta}{\partial r^2} + \frac{1}{r} \frac{\partial \theta}{\partial r} + \frac{\partial^2 \phi}{\partial r^2} + \frac{1}{r} \frac{\partial \phi}{\partial r} \right\} &= c_k(\theta_{k-1} + \phi_{k-1}) \\
 + a_k(\theta_k + \phi_k) + b_k(\theta_{k+1} + \phi_{k+1}) &= \frac{\partial \theta}{\partial \tau} = \frac{\theta_k - \phi_k}{\Delta\tau} \quad (A.5)
 \end{aligned}$$

Thus, grouping the unknown terms on the left hand side the finite difference form of Equation (A.1) is

$$c_k\theta_{k-1} + a_k\theta_k + b_k\theta_{k+1} = d_k \quad (A.6)$$

where

$$\begin{aligned}
 c_k &= -\frac{(3r_k-r_{k+1})(r_{k+1}-r_k)}{2r_k(r_{k+1}-r_{k-1})(r_{k+1}-r_k)(r_k-r_{k-1})} \\
 b_k &= -\frac{(3r_k-r_{k-1})(r_k-r_{k-1})}{2r_k(r_{k+1}-r_{k-1})(r_{k+1}-r_k)(r_k-r_{k-1})}
 \end{aligned}$$

$$a_k = -\frac{(4r_k - r_{k-1} - r_{k+1})(r_{k+1} - r_{k-1})}{2r_k(r_{k+1} - r_{k-1})(r_{k+1} - r_k)(r_k - r_{k-1})} + \frac{1}{\Delta\tau}$$

$$d_k = -c_k \phi_{k-1} + (-a_k + \frac{2}{\Delta\tau})\phi_k - b_k \phi_{k+1}$$

If  $\phi_k$  is known for  $k = 1, 2, \dots, n$  where  $r_n$  is the radius of the interfacial surface at time  $\tau - \Delta\tau$ , Equation (A.6) is applicable for  $k = 2, 3, \dots, n-1$ . At the inner boundary an imaginary node is assumed such that

$$r_2 - r_1 = r_1 - r_0 \quad (A.7)$$

and the inner boundary condition is expressed in finite difference form:

$$\frac{\phi_2 - \phi_0}{2(r_2 - r_1)} = \frac{\theta_2 - \theta_0}{2(r_2 - r_1)} = 1. = \frac{\partial\theta}{\partial r} \quad (A.8)$$

substitution of Equations (A.7) and (A.8) into Equation (A.6) for  $k = 1$  yields the equation for the inner boundary:

$$\left\{ \frac{1}{(r_2 - r_1)^2} + \frac{1}{\Delta\tau} \right\} \theta_1 - \frac{1}{(r_2 - r_1)^2} \theta_2 = \frac{1}{(r_2 - r_1)^2} (\phi_2 - \phi_1) + 1. - \frac{2}{r_2 - r_1} + \frac{\phi_1}{r_2 - r_1} \quad (A.9)$$

For  $k = n$  Equation (A.4) is not valid for  $\phi$  since  $\frac{\partial\phi}{\partial r}$  is not defined at  $r_n$ . Instead, from Equation (A.1)

$$\frac{\partial^2 \phi_n}{\partial r^2} + \frac{1}{r} \frac{\partial \phi_n}{\partial r} = \frac{\partial \phi_n}{\partial \tau} = \frac{\partial \phi_n}{\partial r} \frac{\partial r_n}{\partial \tau} = \frac{\partial \phi_n}{\partial r} \frac{\partial \ell}{\partial \tau}$$

and from Equation (15)

$$\frac{\partial \phi_n}{\partial r} = \frac{1}{2S_{Te}} \frac{\partial \ell}{\partial \tau}$$

so that, in finite difference form

$$\frac{\partial^2 \phi_n}{\partial r^2} + \frac{1}{r} \frac{\partial \phi_n}{\partial r} = \left( \frac{\ell - r_n}{\tau_{n+1} - \tau_n} \right)^2 / 2 S_{Te} \quad (A.7)$$

and substitution into Equation (A.5) yields

$$c_n \theta_{n-1} + a_n \theta_n = \frac{(\ell - r_n)^2}{(\tau_{n+1} - \tau_n)^2} / 2 S_{Te} + \frac{\phi_n}{\Delta \tau} \quad (A.8)$$

where  $c_n$  and  $a_n$  are given by Equation (A.6) with  $\ell$  used for  $r_{k+1}$ .

## APPENDIX B

### PROGRAM ICE2

This appendix documents the program ICE2 which finds the temperature distribution and interface radius for the axisymmetric system using the temperature formulation developed in Section V.2.b. Figure B-1 is a program listing. Figure B-2 shows the necessary control cards and sample input data to run the program. The input is organized as follows:

Record 1 has a format of 5E12.0 and contains the following variables

DIF - diffusivity of thermal storage material,  $\text{ft}^2/\text{hr}$   
CON - thermal conductivity of thermal storage material,  $\text{BTU}/\text{ft}\cdot\text{hr}\cdot{}^{\circ}\text{F}$   
DEN - density of thermal storage material,  $\text{lbf}/\text{ft}^3$   
TF - fusion temperature of thermal storage material,  ${}^{\circ}\text{F}$   
HSL - latent heat of fusion of thermal storage material,  $\text{BTU}/\text{lbf}$

Record 2 has a format of 5E12.0 and contains the following variables

RI - outer radius of heat pipe wall, ft  
RO - inner radius of outer canister wall, ft  
QR - heat flux rate at outer heat pipe wall,  $\text{BTU}/\text{ft}^2\text{hr}$   
DNR - ratio of solid salt volume to canister volume  
DT - time between successive calculations,  $\frac{\alpha_f\Delta t}{R_I^2}$

Record 3 has a format of 4E12.0 and contains the following variables

DFF - canister wall diffusivity,  $\text{ft}^2/\text{hr}$   
CFN - canister wall conductivity,  $\text{BTU}/\text{ft}\cdot\text{hr}\cdot{}^{\circ}\text{F}$   
DFN - canister wall density,  $\text{lbf}/\text{ft}^3$   
P - canister wall thickness, ft

Record 4 has a format of E12.0, 3I5 and contains the following variables

EPS - tolerance on calculation of energy integral  
IP - print every IPth time calculations are made  
L - if L = 1 output is dimensionless otherwise it is dimensional  
ICN - case number for identification

PROGRAM ICE2 74/74 CFI=1 FTI 4.6+446

```
PROGRAM ICE2(INPUT,OUTPUT,TAPE2=OUTPUT)
DIMENSION S(100)
COMMON PT(100),TNT,B(100),SUB(100),SUP(100),D(100),RH(100),E(100).
1F
READ 100, DIF,CON,BEN,TF,HSL
READ 100, PI,RO,GF,JNK,DT
READ 100,DFF,CFN,DFN,F
READ 500, EPS,EP,L,TCN
DO 40 I=1,50
B(I)=0.
40
BT(I)=0.
I0=IP
RMAX=SQRT(DEN+0*F+((1.-DEN)*RI*RI)/RI)
RI=GR*RI/CON
F=GR*RI/DIF/CON/HSL
TNT=DT
DELT=TF+ALOG(TI/(RI-F))
T(1)=1.
S(1)=PI
I0=1.
L=3.*F/(4.+2.*F)
WRITE(2,550)
IF(L.EQ.1)GO TO 55
WRITE(2,650)I0N
GO TO 55
55
WRITE(2,600)TCN
65
DT=DT*100
WRITE(2,700)QR,LNR,TR,TF,RI,RO,F
WRITE(2,750)DEN,CON,DIF,HSL,DFN,CFN,DFF
WRITE(2,800)DELT
DT=DT/100
DO 50 I=1,50
T(2)=SQRT(1.+2L*(DT+ALOG(DT)/2.))
IF (ABS(R(2)-FG).LT.1.E-6*FG) GO TO 60
RG=R(2)
50
CONTINUE
60
CONTINUE
S(2)=R(2)+I
R(1)=ALOG(R(1)/R(2))
C(1)=1./(R(2)-R(1))/L.(R(2)-R(1))
NDF(1)=-C(1)
E(1)=C(1)-(R(2)-R(1))+1.-2./(R(2)-R(1))
T=2
DTG=(1.-R(2)+R(1))/4.+ALOG(-R(2))/2.
DT=DTG
TF=1.3+DT
10
YF=SQRT(1.+2.*F*(TF+L*G))
ZFL=DFUN(YF,TF,DT,DRFG)
IF ((TF*(DTG-DRFG)).LT.-DRFG*EPS) GO TO 70
DT=DTG
GO TO 10
```

Figure B-1. Program ICE2

```

70  IF (YF.LT.1.01*MAX+.01*(YP-R(NT))) GO TO 80
    P=T, T+(RM/X-1(NT))/((YP-R(NT))*ITF-TNT)
    C=IP
    GO TO 10
10  P(NT+1)=YF
    S(NT+1)=R(NT+1)*R1
    DC 20 I=2,NT
20  FH(I)=-SUB(I)*B(I-1)+D(I)*B(I)+SUP(I)*B(I+1)
    NT=NT+1
    DC 30 I=1,NT
    PT(I)=P(I)
    IF (AC.LT.1P) GO TO 50
    1E=1E+1,I=1/DIF
    IF (L.EQ.1) GO TO 35
    WRITE (2,200) T4,S(NT)
    W-ITF (2.400)
15  DC 5 I=1,NT
5   B(I)=1E+7E+3(I)
    IF (L.EQ.1) GO TO 45
    WRITE (2,300) (S(I),E(I),I=1,NT)
25  DC=0
    IF (T.E.LT.2.01*CT) IC=2
50  IC=DC+1
    T2=TC+CT
    T3=TC+CT
    IF (YF.LT.1.01*(P(NT)-P(NT-1))) GO TO 10
100  FO M,1 (5E12.0)
200  FO M,1 (FH TIME=,F15.6,2HHR,/,," RADIUS OF LIQUID/SOLID INTERFACE=,
    1.5E+8,2HET)
250  FO M,1 (//,6H TIME=,F5.5,22X,17HWALL TEMPERATURE=,
    1E+7,/,1H ,11X,*RADIUS OF LIQUID/SOLID INTERFACE=*,F9.6)
300  FO M,1 (15(1H ,F0.4,F0.2,F0.2,F0.4,F0.2,F0.4,F0.2,/,))
350  FO M,1 (15(1H ,F8.4,F8.4,F8.4,F8.4,F8.4,F8.4,F8.4,/,))
400  FO M,1 (1F ,4(16H RAD,FT TEMP,FT))
450  FO M,1 (1H0,4(16H RAD TEMP ))
500  FO M,1 (F12.0,3I5)
550  FO M,1 (1H1,5X,*HEAT TRANSFER IN PHASE CHANGE/THERMAL ENERGY STORE,
    1GE SYSTEM*)
600  FO M,1 (//,1H ,*SYMMETRIC TEMPERATURE FORMULATION-CASE NO*,I3,*
    1 DIMENSIONLESS OUTPUT *)
650  FO M,1 (//,1H ,* SYMMETRIC TEMPERATURE FORMULATION-CASE NO*,I3,*
    1 DIMENSIONAL OUTPUT*)
700  FO M,1 (1E0,* HEAT FLUX RATE=*,F10.3," STU/FT**2-HR FILLED V
    1E0 F=*.F0.2,* PEFCET=*,//.1E0,* TERENCE TEMPERATURE=*,F7.2,* F 1
    1IT/1L/FUSION TEMPERATURE=*,F1.2,2H F,///,1H ,26Y,* CANNISTER GEOME
    1 Y=,//,1F ,22X,*1E 1E ,* TUSE=*,F10.4,3H F7,/,1H ,22X,
    1E USE ,*2E 1E ,*F10.4,3H F7,/,1H 0.20X,*WALL THICKNESS=*,F10.4,
    13H F7,/,1H ,27X,* THERMAL STURGE MATERIALS & PROPERTIES*)
750  FO M,1 (//,1H ,27X,* CENSITY=*,F10.4," LB/FT**3,/,1H0,14X,* THERM
    1L CONDUCTIVITY=*,F10.6," BTU/H-FT-F*,/,1H0,15X,* THERMAL DIFFUSIV
    1*Y=*,F10.7," FT**2/HR",/,1H0,13Y,* LATENT HEAT OF FUSION=*,F10.4,*,
    1E TUR/1L*,/,1H ,20X,* CANNISTER MATERIAL PROPERTIES=/,1H ,27X,
    1E STY=*,F10.4," LB/FT**3,/,1H0,14X,* THERMAL CONDUCTIVITY=*,F10
    1E ,* BTU/H-FT-F*,/,1H0,15X,* THERMAL DIFFUSIVY=*,F10.7," FT**2/H
    1")

```

THIS PAGE IS BEST QUALITY ERASABLE

THIS COPY PUBLISHED TO DDC

```

100  ED:R= (//,1H ,10X,***ER,4*U-F 20000 (4*10000) 10000,FG.0
1,* FG,/,1H1)
      STOP
25  WRITE(2,250) TP,PT(1),T(NT)
      WRITE(2,450)
      GO TO 15
45  WRITE(2,350) (-_),P1(I),I=1,NT)
      GO TO 25
      END

```

SUBROUTINE DFUN(YF,TF,NT,DF,RG)

```

COMMON PT(100),INT,B(100),SUP(100),D(100),RH(100),R(100),
1F
      RG=0 (NT)
      RL=0 (NT-1)
      DT=.5/ (FG*(YP-FG)*(RG-RL)*(YF-RL))
      SUB(NT)=-DT*(YF-FG)*(3.*RG-YF)
      S(NT)=DT*(YP-RL)*(4.*FG-YP-RL)
      SUP(NT)=-DT*(RG-RL)*(3.*FG-RL)
      CH(NT)=((YF-FG)/(TP-NT))/**2/2./F
      DO 10 I=1,NT
      D(I)=D(I)+1./(F-NT)
10      B(I)=PT(I)+PT(I)/(TP-NT)
      CALL 1,10 (SUP,1,DF,B,NT)
      D=0.
      DO 20 I=2,NT
20      DN:G=D*RG+B(I)+B(I-1)+K(I-1)*(E(I)-E(I-1))/2.
      DN:G=DN:G+P(NT)*K(NT)*(YP-F(NT))/2.
      RETURN
      END

```

SUBROUTINE TRTL(DUB,DIA,SUP,B,N)

```

SI ER1000, SUE(100), DIA(100), SUP(100), E(100)

```

```

IF(M.GT.1) GO TO 10

```

```

B(1)=B(1)/E(1)

```

```

-ER1000

```

```

10  DO 20 K=2,N

```

```

  E(K)=-DUE(K)/DIA(K-1)

```

```

  DIA(K)=DIA(K)+K**2*SUP(K-1)

```

```

20  B(K)=E(K)+PAT*B(K-1)

```

```

  E(N)=E(N)/DIA(N)

```

```

  K=N

```

```

  DO 30 KD=2,N

```

```

  K=K-1

```

```

30  B(K)=(B(K)-SUP(K)*B(K+1))/DIA(K)

```

```

  RETURN

```

```

  END

```

UD121,T15,I010,CM60000,STCSA.P740579,BANDOW,KL121,229-2835  
COMMENT.\*\*\*\*\*NO DECK\*\*\*\*\*  
COMMENT.\*\*\*\*\*93392\*\*\*\*\*  
ATTACH,F,ICE,CY=1.  
FTN,I=F,L,R=3,B=FLGO.  
RETURN,F.  
REWIND,FLGO.  
FLGO,PL=20000.  
\*EOR  
    .035       4.11       181.       1310.       350.  
    .0625       .1195833    8691.133    .7056356   .095800525  
    .2244971      13.5       501.12      .005416667  
    .0001        1        1        0  
\*EOR  
\*EOF

Figure B-2  
Control Cards

THIS PAGE IS BEST QUALITY PRACTICALLY  
FROM COPY PUBLISHED TO DDC

## APPENDIX C

### PROGRAM ENTH

This appendix documents the program ENTH which calculates the axisymmetric temperature distribution and interface radius from the enthalpy formulation developed in Section VI.1.a. Figure C-1 is a program listing, Figure C-2 shows the control cards and sample input data. The input is organized as follows:

Record 1, format 5E12.0

DIF - thermal diffusivity of thermal storage material,  $\text{ft}^2/\text{hr}$

CON - thermal conductivity of thermal storage material,  $\text{BTU}/\text{ft}\cdot\text{hr}\cdot{}^{\circ}\text{F}$

DEN - density of thermal storage material,  $\text{lbm}/\text{ft}^3$

TF - fusion temperature of thermal storage material,  ${}^{\circ}\text{F}$

HSL - latent heat of fusion of thermal storage material,  $\text{BTU}/\text{lbm}$

Record 2, format 5E12.0

RI - outer radius of heat pipe wall, ft

RO - inner radius of outer canister wall, ft

QR - heat flux rate at outer edge of heat pipe,  $\text{BTU}/\text{ft}^2\text{hr}$

DNR - ratio of solid thermal storage material volume to canister volume

ERR - allowable error in enthalpy change

Record 3, format 4E12.0

ORF - relaxation factor effects speed of convergence

DFF - thermal diffusivity of canister wall,  $\text{ft}^2/\text{hr}$

CFN - conductivity of canister wall,  $\text{BTU}/\text{ft}\cdot\text{hr}\cdot{}^{\circ}\text{F}$

DFN - density of canister wall,  $\text{lbm}/\text{ft}^3$

Record 4, format 7I5

NR - number of nodes in radial direction in salt

NT - number of points in time

IM - maximum number of iterations allowed  
IP - print every IPth time  
IR - dummy variable  
IF - number of nodes in radial direction in wall  
ICN - case number for identification

06-24-86 EFT 4 - 74/74 - CPT=1 EFT= 4.6+446

Figure C-1. Program ENTH

```

IF (I.LE.IF) OF=OFF
IF (I.LT.IF) CN1=CFN/CON
IF (I.LE.1F)-CN2=CFN/CON
IF (I.EQ.IF) CN1=2.*CON*CFN/(CON+CFN)/CON
IF (I.EQ.IF+1) CN2=2.*CON*CFN/(CON+CFN)/CON
H(I)=(D*PH(I)+(1.+C(I))*CN1*T(I+1)+(1.-C(I))*CN2*T(I-1))/(D+(CN1*
1*(1.+C(I))+CN2*(1.-C(I))))/DF
IF (H(I).LT.0.) GO TO 30
H(I)=H(I)*(D+(CN1*(1.+C(I))+CN2*(1.-C(I)))/DF)/D
T(I)=0.
GO TO 40
30 CONTINUE
IF (OH.LT.0.) H(I)=OFF*H(I)+(1.-DF)*OH
T(I)=H(I)/DF
EN=EN+ABS(H(I)-OH)
FO=FO+ABS(H(I))
40 CONTINUE
IF (EN.LT.ED*ERF) GO TO 60
IT=IT+1
IF (IT.LT.IM) GO TO 50
50 IS=IS+1
IC=IC+1
IF (IC.LT.IF) GO TO 5
NM1=NM-1
FF=0.4*IS
FF=(NM-IF-1)*(NM-1).
W1=(CON*T(IF+1)+CFN*T(IF))/(CON+CFN)/ST
TW=(3.*T(1)-T(2))/2./ST
SM=0.
HE=0.
GO TO 15 I=1,4M
HI=1.
IF (I.LE.IF) HI=0.
HJ=AM*X1(0.,H(I))
SM=SM+2.*R(I)*DF*(HI-HJ)
HE=HE+2.*R(I)*DF*(HI-H(I))
15 PH(I)=T(I)/ST
FO=EN/ED
WE=7E-(2,400)-FF,HE,SM,IT,FR,TW,TW1,FF
WRITE (2,500) (F(I),FH(I),I=1,NM1)
IC=0
IF (IS.LE.1) IC=1
60 DO I=1,4M
70 PH(I)=H(I)
IF (IS.LE.AT) GO TO 80
100 FO=1. (5E12.0)
200 FO=1.47454
300 FO=M17 (1H1, 6X, *HEAT TRANSFER IN PHASE CHANGE/ THERMAL ENERGY CT)
14GE-SYSTE*+,//1H+,*SYMMETRIC ENTHALPY FORMULATION-CASE NO*+
1,13,4X,*DIMENSIONLESS OUTPUT*,/,1H0,*HEAT FLUX RATE=*,F10.3,*BT*
1/FT*=2-H2*,6X,*FILLED VOLUME=*,F5.1,*FUGENT*,/,1H0,*REFERENCE*
1*REFAT(1H)=*,F7.2,*F INIT=*,/FUSION TEMPERATURE=*,F5.2,*F2*
1F5.2,2H F,///,1H ,26X,*GAMMISTER GEOMETRY*,/,1H ,22X,*INNER RADI*
18=*,F10.5,3H F*,/,1H0,22X,*OUTER RADIUS=*,F10.5,3H FT,/,1H0,20X

```

1, \*WALL THICKNESS=\*, F10.6, 3H 53, //, 1H , 17X, \*THERMAL STORAGE MATER  
 1(ML PROPERTIES\*)  
 350 FG-MAT -(1H0,27X,\*DENSITY=\*,F10.4," LB/M/FT\*\*3",/1H0,14X,\*THERMAL CON  
 1DUCTIVITY=\*,F10.6," BTU/LB/FT-FT",/,1H0,15X,\*THERMAL DIFFUSIVITY=\*,  
 1",F10.7," FT\*\*2/HR",/,1H0,13X,\*LATENT HEAT OF FUSION=\*,F10.4,\* 3E  
 1/LEM\*,//,1H ,20X,\*CANNISTER MATERIAL PROPERTIES\*,//,1H ,27X,\*DEN  
 SITY=\*,F10.4," LB/M/FT\*\*3",/,1H0,14X,\*THERMAL CONDUCTIVITY=\*,F10.6,"  
 1 BTU/HP-FT-F",/,1H0,15X,\*THERMAL DIFFUSIVITY=\*,F10.7," FT\*\*2/HR")  
 400 FG-MAT -( //,1H ,3X,\*TIME=\*,F12.6,4X,\*HEAT OUT=\*,F9.6,5X,\*SOLID 1  
 1JLUME=\*,F9.6,/,1H ,15X,\*ITERATIONS=\*,15,10X,\*ERRCR=\*,E12.5,/,  
 1H ,\*INNER WALL TEMPERATURE=\*,F9.6,7X,\*OUTER WALL TEMPERATURE=\*,  
 1,F9.6,/,1H ,23X,\*INTERFACE RADIUS=\*,F9.6,/,1H0,\* RADIUS TEMP  
 1 RADIUS TEMP RADIUS TEMP RADIUS TEMP)  
 500 FG-MAT -(13(1H ,8F6.4,/) )  
 450 FG-MAT (//,1H ,10X,14,\* NODES RADIALLY\*,13X,14,\* TIME STEPS\*,//,1  
 1H ,14,\* ITERATIONS - ERROR=\*,E7.1,6X,\*RELAXATION FACTOR=\*,F6.3)  
 STOP  
 END

THIS PAGE IS BEST QUALITY PROGRAMMED  
 FROM COPY PERTINENT TO DOG

UD121,T30,I015,CM60000,STCSA.F740579,BANDOW,KL121,229-2835  
COMMENT.\*\*\*\*\*NO DECK\*\*\*\*\*  
COMMENT.\*\*\*\*\*93392\*\*\*\*\*  
ATTACH,F,ICE,CY=3.  
FTN,I=F,L,R=3,B=FLGO.  
RETURN,F.  
REWIND,FLGO.  
FLGO,FL=20000.  
\*EOR  
      .035      4.11      181.      1310.      350.  
      .0625     .1195833    8691.133    .7056356    .00001  
      1.92      .2244971    13.5      501.12  
      63     160     200     16      1      6      0  
\*EOR  
\*EOF

Figure C-2  
Control Cards

THIS PAGE IS BEST QUALITY PRACTICABLE  
FROM COPY PUBLISHED TO DDC

## APPENDIX D

### PROGRAM FIN

This appendix documents the program FIN used to calculate the temperature distribution and interface radius for the finned HP/TES systems. Figure D-1 is a program listing while Figure D-2 shows the control cards and sample input data. The input data is organized as follows:

Record 1, format 5E12.0

DIF - thermal diffusivity of salt,  $\text{ft}^2/\text{hr}$   
CON - conductivity of salt,  $\text{BTU}/\text{ft}\cdot\text{hr}\cdot{}^{\circ}\text{F}$   
DEN - density of salt,  $\text{lbm}/\text{ft}^3$   
TF - fusion temperature of salt,  ${}^{\circ}\text{F}$   
HSL - latent heat of fusion of salt,  $\text{BTU}/\text{lbm}$

Record 2, format 5E12.0

DFF - diffusivity of canister wall,  $\text{ft}^2/\text{hr}$   
CFN - conductivity of canister wall,  $\text{BTU}/\text{ft}\cdot\text{hr}\cdot{}^{\circ}\text{F}$   
DFN - density of canister wall,  $\text{lbm}/\text{ft}^3$   
QR - heat flux rate at outer edge of heat pipe,  $\text{BTU}/\text{ft}^2\text{hr}$   
DNR - ratio of solid salt volume to canister volume

Record 3, format 5E12.0

RI - outer radius of heat pipe wall, ft  
RO - inner radius of outer canister wall, ft  
B - half thickness of fin, ft  
P - thickness of heat pipe wall, ft  
G - length of fins, ft

Record 4, format 2E12.0

ORF - relaxation factor effecting speed of convergence  
ERR - error tolerance on enthalpy change

Record 5, format 4I5

NR - number of nodes in radial direction  
NT - number of points in time  
NS - number of nodes in angular direction  
NFn - number of fins

Record 6, format 4I5

IM - maximum number of iterations  
IP - print every IPth time calculated  
ID - print diagnostic if ID = 1  
ICN - case number for identification

GE LM FIN 74/74 CP,1=1 FTN 4.6+446 C

```

PROGRAM FIN(INPUT1,TAPE1=INPUT,OUTPUT,TAPE2=OUTPUT)
DIMENSION C1(25,30),C2(25,30),C3(25,30),C4(25,30),C5(25,30),
1PH(25,30),T(25,30),H(25,30),NF(25),F(25),RF(30)
READ (1,100) DIF,CON,DEN,TF,HSL
READ (1,100) DFF,CFN,DFN,DF,DNR
READ (1,100) RI,R0,B,P,G
READ (1,100) OFF,ERX
READ (1,200) NR,NT,NS,NFN
READ (1,200) IM,IP,IE,ICH
IC=IP
IS=0
JP=14
RD=57.295779
RM,X=R0/PI
DF=(R0-PI)/PI/NR
DO=3.14159277/NFN/NS
ST=0.*I/PI/DF/DEN/HSL
DT=(R0+RD-PI*RI)*DNR/2./PI/RI/ST/NT
DELT=DT/DT
FT=PI/DT/PI
TREF=0.4*PI/CON
IF=1LT(FT)
IF (FT-AINT(FT).GT..5) IF=IF+1
N=NR+2*IF
M1=M-1
N=NS
N1=N-1
DFF=DIF*CFN/DFF/CON
DO 10 I=1,M
NF(I)=NS+1
F(I)=1.
IF (I.LE.1F) GO TO 10
IF (I.GT.M-1F) GO TO 10
R=(2.+(I-1F)-1.)/2.*DELT+1.
A=B/R1/R/DO
NF(I)=INT(A)
F(I)=A-INT(A)
IF (I.LT.(RJ+G)/E_) GO TO 10
NF(I)=0
F(I)=0.
CONTINUE
IF (I.LT.1) GO TO 4
WRITE (2,500) RI,PH,BS,ST,LT,D,FT,DFF
WRITE (2,600) IC,IS,IF,M,M1,N,N1
WRITE (2,700) (F(I),I=1,M)
WRITE (2,800) (NF(I),I=1,M)
CONTINUE
DO 20 I=1,M
DO 20 J=1,N

```

Figure D-1. Program FIN

```

C1(I,J)=C2(I,J)=C3(I,J)=C4(I,J)=CON
IF ( J.LE.NF(I) ) C1(I,J)=C2(I,J)=C3(I,J)=C4(I,J)=CFN
IF ( J.EQ.NF(I)+1 ) C1(I,J)=C3(I,J)=(1-F(I))*CON+F(I)*CFN
TF ( J.EQ.NF(I).AND.F(I).LT..5 ) C2(I,J)=CON*CFN/(.5*(CON+CFN))+F(I)
1*(CON-CFN)
IF ( J.EQ.NF(I)+1.AND.F(I).LT..5 ) C4(I,J)=CON*CFN/(.5*(CON+CFN))+F(I)
1*(CON-CFN)
IF ( J.EQ.NF(I)+1.AND.F(I).GE..5 ) C2(I,J)=CON*CFN/(.5*(3.*CFN-CON)+1
1F(I)*(CON-CFN))
IF ( J.EQ.NF(I)+1.AND.F(I).GE..5 ) C4(I,J)=CFN
IF ( J.EQ.NF(I)+2.AND.F(I).GE..5 ) C4(I,J)=CON*CFN/(.5*(3.*CFN-CON)+1
1F(I)*(CON-CFN))
20 CONTINUE
IF ( ID.LT.1 ) GO TO 6
WRITE (2,700) ((C1(I,J),J=1,N),I=1,M)
WRITE (2,700) ((C2(I,J),J=1,N),I=1,M)
WRITE (2,700) ((C3(I,J),J=1,N),I=1,M)
WRITE (2,700) ((C4(I,J),J=1,N),I=1,M)
6 CONTINUE
DO 30 I=1,M
R=1.+(2.* (I-IF)-1.)/2.*DR
DO 30 J=1,N
IF ( J.EQ.M ) GO TO 40
C1(I,J)=2.*C1(I,J)*C3(I+1,J)/(C1(I,J)+C3(I+1,J))
C3(I+1,J)=C1(I,J)
40 C1(I,J)=C1(I,J)/CON*(1.+DR/2./R)
C2(I,J)=C2(I,J)*(DR/R/DS)**2./CON
C3(I,J)=C3(I,J)/CON*(1.-DR/2./R)
C4(I,J)=C4(I,J)*(DR/R/DS)**2./CON
IF ( I.EQ.1 ) C3(I,J)=0.
IF ( J.EQ.1 ) C4(I,J)=0.
IF ( I.EQ.M ) C1(I,J)=0.
IF ( J.EQ.N ) C2(I,J)=0.
FF=0.
IF ( J.LE.NF(I) ) FF=1.
IF ( J.EQ.NF(I)+1 ) FF=F(I)
C5(I,J)=0+(C1(I,J)+C2(I,J)+C3(I,J)+C4(I,J))/(1.-FF*(1.-DFR))
T(I,J)=0.
PH(I,J)=1.
IF ( J.LE.NF(I) ) PH(I,J)=0.
IF ( J.EQ.NF(I)+1 ) PH(I,J)=1.-F(I)
H(I,J)=PH(I,J)
30 CONTINUE
IF ( ID.LT.1 ) GO TO 7
WRITE (2,700) ((C1(I,J),C2(I,J),C3(I,J),C4(I,J),C5(I,J),
1J=1,N),I=1,M)
WRITE (2,700) ((H(I,J),J=1,N),I=1,M)
WRITE (2,700) ((PH(I,J),J=1,N),I=1,M)
7 CONTINUE
DN=DN*100
WRITE (2,300) ICH,RFN,QR,DRN,L,NFN,RI,B,RO,G
DN=DN/100
WRITE (2,350) DEM,DFN,CON,CFN,DIF,DFF,HSL,M,N,NT,DRF,ERF,IM
WRITE (2,360) TREF,-F,ST

```

```

60  IT=0
95  DO 6 J=1,N
8  RF(J)=0.
OH=H(1,1)
H(1,1)=(D*FH(1,1)+C1(1,1)*T(2,1)+C2(1,1)*T(1,2)-DR*ST)/C5(1,1)
H(1,1)=DRF*(H(1,1)-OH)+OH
T(1,1)=H(1,1)/DFR
EN=ABS(H(1,1)-OH)
ED=ABS(H(1,1))
DO 50 I=2,M1
OH=H(I,1)
H(I,1)=(D*FH(I,1)+C1(I,1)*T(I+1,1)+C2(I,1)*T(I,2)+C3(I,1)*T(I-1,1))/C5(I,1)
IF (H(I,1).LT.0.) GO TO 60
H(I,1)=H(I,1)*C5(I,1)/D
T(I,1)=0.
IF (RF(I).LT.1.) RF(I)=(I-IF-H(I,J))*DR+1.
GO TO 50
60  IF (OH.LT.0.) H(I,1)=DRF*(H(I,1)-OH)+OH
FF=F(I)
IF (NF(I).GT.0) FF=1.
T(I,1)=H(I,1)/(1.-FF*(1.-DFR))
EN=EN+ABS(H(I,1)-OH)
ED=ED+ABS(F(I,1))
50  CONTINUE
CH=H(M,1)
H(M,1)=(D*FH(M,1)+C2(M,1)*T(M,2)+C3(M,1)*T(M-1,1))/C5(M,1)
IF (H(M,1).LT.0) GO TO 90
H(M,1)=H(M,1)*C5(M,1)/D
T(M,1)=0.
GO TO 70
50  IF (CH.LT.0.) H(M,1)=DRF*(H(M,1)-OH)+OH
T(M,1)=H(M,1)/DFR
EN=EN+ABS(H(M,1)-OH)
ED=ED+ABS(H(M,1))
70  CONTINUE
DO 5 J=2,N1
OH=H(1,J)
H(1,J)=(D*FH(1,J)+C1(1,J)*T(2,J)+C2(1,J)*T(1,J+1)+C4(1,J)*T(1,J-1)
1-S1)/C5(1,J)
H(1,J)=DRF*(H(1,J)-OH)+OH
T(1,J)=H(1,J)/DFR
EN=EN+ABS(H(1,J)-OH)
ED=ED+ABS(H(1,J))
DO 15 I=2,M1
CH=H(I,J)
H(I,J)=(D*FH(I,J)+C1(I,J)*T(I+1,J)+C2(I,J)*T(I,J+1)
1+C3(I,J)*T(I-1,J)+C4(I,J)*T(I,J-1))/C5(I,J)
IF (H(I,J).LT.0) GO TO 25
H(I,J)=H(I,J)*C5(I,J)/D
T(I,J)=0.
IF (RF(J).LT.1.) FF(J)=(I-IF-H(I,J))*DR+1.
GO TO 15

```

```

25    IF (CH.LT.0.) H(I,J)=(H(I,J)-OH)*DRF+OH
      FF=0.
      IF (J.LE.NF(I)) FF=1.
      IF (NF(I)+1.EQ.J) FF=F(I)
      T(I,J)=H(I,J)/(1.-FF*(1.-DFR))
      EN=EN+ABS(H(I,J)-OH)
      ED=ED+ABS(H(I,J))
15    CONTINUE
      OH=H(M,J)
      H(M,J)=(D*FH(M,J)+C2(M,J)*T(M,J+1)+C3(M,J)*T(M-1,J)
      +C4(M,J)*T(M,J-1))/C5(M,J)
      IF (H(M,J).LT.0.) GO TO 45
      H(M,J)=H(M,J)*C5(M,J)/D
      T(M,J)=0.
      GO TO 35
45    IF (OH.LT.0.) H(M,J)=DRF*(H(M,J)-OH)+OH
      T(I,J)=H(M,J)/DFR
      EN=EN+ABS(H(M,J)-OH)
      ED=ED+ABS(H(M,J))
35    CONTINUE
5     CONTINUE
      OH=H(1,N)
      H(1,N)=(D*FH(1,N)+C1(1,N)*T(2,N)+C4(1,N)*T(1,N-1)
      +C5(1,N))/C5(1,N)
      H(1,N)=0-F*(H(1,N)-OH)+OH
      T(1,N)=H(1,N)/DFR
      EN=EN+ABS(H(1,N)-OH)
      ED=ED+ABS(H(1,N))
      DO 55 I=2,M1
      OH=H(I,N)
      H(I,N)=(D*FH(I,N)+C1(I,N)*T(I+1,N)+C3(I,N)*T(I-1,N)
      +C4(I,N)*T(I,N-1))/C5(I,N)
      IF (H(I,N).LT.0.) GO TO 65
      H(I,N)=H(I,N)*C5(I,N)/D
      T(I,N)=0.
      IF (RF(N).LT.1.) RF(N)=(I-IF-H(I,N))/DF+1.
      GO TO 55
65    IF (OH.LT.0.) H(I,N)=C*F*(H(I,N)-OH)+OH
      FF=0.
      IF (NF(I).GE.N) FF=1.
      T(I,N)=H(I,N)/(1.-FF*(1.-DFR))
      EN=EN+ABS(H(I,N)-OH)
      ED=ED+ABS(H(I,N))
55    CONTINUE
      OH=H(M,N)
      H(M,N)=(D*FH(M,N)+C3(M,N)*T(M-1,N)+C4(M,N)*T(M,N-1))/C5(M,N)
      T(M,N)=H(M,N)/DFR
75    CONTINUE
      IF (EN.LT.ED+ERR) GO TO 35
      IT=IT+1
      IF (IT.LT.IIM) GO TO 35
85    IS=IS+1
      IC=IC+1
      IF (IC.LT.IP) GO TO 2
      SM=0.

```

```

HE=0.
DO 1 I=1,M
I=1.+(I-IF-.5)*DR
DO 1 J=1,N
HI=1.
IF (J.LE.NF(I)) HI=0.
IF (J.EQ.NF(I)+1) HI=F(I)
HJ=AMAX1(0.,H(I,J))
SM=SM+*DS*DR*(HI-HJ)
HE=HE+F*DS*DR*(HI-H(I,J))
1 PH(I,J)=T(I,J)/ST
ER=EN/ED
TP=DT*IS
SM=SM*2.*NFN /3.1415927
HE=HE*2.*NFN/3.1415927
RE=SCRT(1.+SM)

W=17E (2,400) TF,FE,HE,SM,IT,ER
J1=1
13 J2=J1+JP
J2=AMIN0(J2,N)
WRITE (2,450) (RF(J),J=J1,J2)
DO 9 J=J1,J2
RF(J)=(J-.5)*DS*ED
WRITE (2,500) (RF(J),J=J1,J2)
DO 11 J=J1,J2
11 RF(J)=(3.+T(1,J)-T(2,J))/2./ST
WRITE (2,550) (FF(J),J=J1,J2)
DO 14 J=J1,J2
14 RF(J)=(CON*T(IF+1,J)+CFN*T(IF,J))/(CON+CFN)/ST
WRITE (2,750) (RF(J),J=J1,J2)
WRITE (2,600)
DO 12 I=1,M
M=1.+(I-IF-.5)*DR
12 WRITE (2,650) E,(PH(I,J),J=J1,J2)
J1=J2+1
IF (J1.LE.F) GO TO 13
IC=0
IF (IS.LE.1) IC=1
2 DO 3 I=1,M
3 DO 3 J=1,N
3 PH(I,J)=H(I,J)
IF (IS.LT.FT) GO TO 60
100 FORMAT (5E12.0)
200 FORMAT (5I5)
300 FORMAT (1H1,/,2(1H0,/,1H ,34X,*HEAT TRANSFER IN PHASE CHANGE/THE
1HAL ENERGY STORAGE SYSTEM*,/,1H0,35X,*CASE NUMBER*,13,* DIMENS
10LESS OUTPUT*,110,* FINS*,/,1H0,25X,*HEAT FLUX RATE (BTU/FT**2/H
1)=*,F10.3,11X,*F ALLEE VOLUME=*,F5.1,* PERCENT*,//,1H0,37X,* CANN
1STEF GEOMETRY*,22X,*FIN GEOMETRY*,/,1H0,32X,*WALL THICKNESS,FT=*,1
110.8,12X,*NUMBER OF FINS=*,13,/,1H0,34X,*INNER RADIUS,FT=*,F10.5,
10X,*FIN THICKNESS,FT=*,F10.8,/,1H0,34X,*OUTER RADIUS,FT=*,F10.8,1.

```

THIS PAGE IS BEST QUALITY AVAILABLE  
FROM COPY PUBLISHED IN MAG

```

1X,*FIN LENGTH,FT=*,F10.6)
350 FORMAT (///,1H ,56X,* MATERIAL PROPERTIES*,//,1H0,39X,*PROPERTY*
1,20X,*PHASE CHANGE RATE,IN*,4X,*CANNISTER MATERIAL*,/,1H0,27X,
1*UNITS*,Y,LE4/F1**3",30X,F3.3,15X,F3.3,/,1H0,27X,*THERMAL CONDUCTI-
1I,Y,3TU/FT/Hr/F*,15X,F8.5,15X,F8.4,/,1H0,27X,"THERMAL DIFFUSIVITY
1FT**2/HR",25X,F8.6,15X,F8.6,/,1H0,27X,*LATENT HEAT OF FUSION,BTU/
1BM*,12X,F8.3,/,1H ,52X,*ITERATION CONTROL PARAMETERS*,//,1H ,5X
1*NODAL STRUCTURE*,I5,* NODES RADIALL*,I5,* ANGULAR NODES*,I5,* 
1*TIME STEPS*,/,1H0,5X,*ITERATION PARAMETERS*   OVER-RELAXATION FACT
10E=*,F6.3,5X,*ERROR TOLERANCE=*,E12.4,*   MAXIMUM ITERATIONS=*,I5
360 FORMAT (///,1H ,5X,*REFERENCE TEMPERATURE,F=*,F8.3,11X,*FUSION/IR
1INITIAL TEMPERATURE,F=*,F9.3,12X,*STEFAN NUMBER=*,F12.3)
400 FORMAT (1H1,*TIME=*,F8.4,3X,*EFF RADIUS=*,F9.6,3X,*HEAT EXTRACTED=
1*,F9.6,3X,*SOLID VOLUME=*,F9.6,3X,*ITERATIONS=*,I4,3X,
1*ERROR=*,E12.5)
450 FORMAT (1H0,* S/L RADIUS*,15F8.4)
500 FORMAT (1H ,*FIN UL ANGLE*,15F8.1)
550 FORMAT (1H ,*ID WALL TEMP*,15F8.4)
600 FORMAT (1H ,6X,*RADIUS*,20X,*NODAL DIMENSIONLESS TEMPERATURES
1-TF)/TR*)
650 FORMAT (1H ,4X,16F8.4)
700 FORMAT (1H ,15F8.4)
750 FORMAT (1H ,*ID WALL TEMP*,15F8.4)
800 FORMAT (1H ,10E12.5)
850 FORMAT (1H ,15I5)
STOP
END

```

THIS PAGE IS BEST QUALITY FAXABLE  
FROM COPY FURNISHED TO DDCI

UD121,T200,I030,CM60000,STCSA,P740579,BANDOW,KL121,229-2835  
COMMENT.\*\*\*\*\*NO DECK\*\*\*\*\*  
COMMENT.\*\*\*\*\*93392\*\*\*\*\*  
ATTACH,F,FIN,CY=1.  
FTN,I=F,L,R=3,B=FLGO.  
RETURN,F.  
REWIND,FLGO.  
FLGO,PL=20000.  
\*EOR  
    .035          4.11          181.          1310.          350.  
    .2244971      13.5          501.12      8691.133      .7056356  
    .0625         .1195833     .002604167   .005416667     .05447917  
    1.93          .00001  
    21    80    30    6  
    200    8    0    20  
\*EOR  
\*EOF

Figure D-2  
Control Cards

THIS PAGE IS BEST QUALITY FROM ORIGINAL  
FROM COPY SUBMITTED TO DRG

## REFERENCES

1. Carslaw, H. S., Conduction of Heat in Solids, 2nd Ed., pp. 282-296, Oxford at the Clarendon Press.
2. Kreith, F. and Romie, F. E., "A Study of the Thermal Diffusion Equation with Boundary Conditions Corresponding to Solidification or Melting of Materials Initially at the Fusion Temperature," Proc. Phys. Soc. LXVIII, 5-B, pp. 277-291, 1954.
3. Sfeir, A. A. and Clumpner, J. A., "Continuous Casting of Cylindrical Ingots," ASME Journal of Heat Transfer, pp. 29-34, February 1977.
4. Koeger, P. G. and Ostrach, S., "The Solution of a Two-Dimensional Freezing Problem Including Convection Effects in the Liquid Region," Int. J. Heat Mass Transfer, Vol. 17, pp. 1191-1207, 1974.
5. Cullom, R. R., Diedrich, G., and Albers, L. U., Analysis of Solidification in Thermal-Energy Storage Systems with Axisymmetric Heat-Transfer Solutions, NASA TN D-3763, December 1966.
6. Shamsunder, N. and Sparrow, E. M., "Analysis of Multidimensional Condition Phase Change Via the Enthalpy Model," ASME Journal of Heat Transfer, pp. 333-340, August 1975.